Neutral currents in low-energy nuclear-physics processes

O. Dumitrescu
International Centre for Theoretical Physics, Trieste, Italy;
Department of Theoretical Physics, Institute of Physics and Nuclear Engineering, Institute of Atomic Physics, Măgurele, P.O. Box MG-6, R-76900, Bucharest, Romania

Fiz. Élem. Chastits At. Yadra **27**, 1543–1606 (November–December 1996)

The possibility of extracting from experiment the necessary information concerning the neutral-current contributions to the structure of the weak interactions that violate the parity-conservation law is investigated. The parity nonconservation (PNC) induced by weak hadron–hadron interactions investigated via low-energy nuclear-physics processes is reviewed. The low-energy nuclear-physics processes considered here are resonance nuclear scattering and reactions induced by polarized projectiles such as protons and deuterons, emission of polarized gamma rays from oriented and nonoriented nuclei, and parity-forbidden alpha decays. Some comments on the PNC nucleon–nucleon (PNC-NN) interaction are presented. Explicit expressions for some PNC observables are rederived. Applications for specific scattering, reaction, and decay modes are given. New experiments are proposed. © *1996 American Institute of Physics.* [S1063-7796(96)00106-4]

1. INTRODUCTION

The existence of neutral currents other than the familiar electromagnetic currents was predicted as early as 1958 by Bludman,[1] who constructed a model based on a local SU(2) gauge symmetry. This model incorporated both the charged (entering the β-decay interaction) and neutral currents. The space-time structure of the neutral currents in this first model was of a pure vector minus axial-vector (V−A) type. Thus, they could not be identified with the electromagnetic currents, which are of a pure vectorial and parity-conserving type. There was no unification with electromagnetism in Bludman's model. A model truly unifying weak and electromagnetic interactions incorporating two kinds of neutral currents (electromagnetic and weak) was invented by Glashow[2] and by Salam and Ward.[3] This model is the SU(2)⊗U(1) model. As it is stated in this last model, there is no mechanism for the mass generation of the intermediate vector bosons. Thus, the relative strength of weak neutral-current interactions to that of charged-current interactions is a completely free parameter. This problem was settled by Weinberg,[4] who incorporated the idea of spontaneous breakdown of local gauge symmetry[5,6] into the SU(2)⊗U(1) model. An analogous mechanism was proposed by Salam.[7] The mass of the intermediate boson (Z) that mediates the neutral current is related in a definite way to the mass of its charged counterpart (W). The above relative strength was therefore fixed once and for all in this version of the SU(2)⊗U(1) model, predicting in this way the structure of the weak neutral currents (as a mixture of vector and axial-vector currents) and its strength of interaction. Thus, the SU(2)⊗U(1) model became a single-parameter ($\sin^2\theta_W$) theory. With the discovery of neutral current in 1973,[8] this standard SU(2)⊗U(1) field theory stood out as a strong candidate for a unique theory of electroweak interactions. In the following years great progress was made in understanding the weak NN interactions, especially after the experimental detection[9,10] of $W^{\pm}$ and Z^0 bosons, the mediators of the weak force.

The weak interactions between the nucleons, and especially those components with a dominant contribution of the neutral currents, can be studied only when the strong and electromagnetic interactions between the nucleons are forbidden by a symmetry principle, such as flavor [i.e., strangeness (S) or charm (C)] conservation. According to the standard theory, the neutral-current contributions to $\Delta S=1$ and $\Delta C=1$ weak processes are strongly suppressed[11,12] and, therefore, the neutral-current weak interaction between quarks can only be studied in flavor-conserving processes which can be met in low-energy nuclear-physics processes. The isovector part of the charged-current weak interaction is suppressed by $\tan^2\theta_C$,[11,12] where θ_C is the Cabibbo angle; therefore, the isovector part of the weak interaction contains mainly the neutral currents. Thus, the PNC nuclear-physics processes determined by an isovector parity-mixed doublet are very important for studies of the neutral currents.

The search for parity nonconservation (PNC) in complex nuclei, and especially in cases where an enhanced effect is expected from the existence of parity-mixed doublets (PMD),[13–41] has a long history. The enhancement of any PNC effect is predicted by several factors, the most important being the small level spacing between states of the same spin and opposite parity in the compound nucleus involved. The second one arises from the expected increase of the ratio (f) between parity-forbidden and parity-allowed transition matrix elements caused by the nuclear structure of the states involved. Usually, such enhancements are offset by correspondingly large theoretical uncertainties in the extraction of the PNC-NN parameters from the experimental data. As a matter of fact, the same conditions which generate the enhancement complicate a reliable determination of the nuclear matrix elements, theoretically. Therefore, it is necessary to select exceptional cases, in which the nuclear-structure problem can be solved. This is the case for closely spaced doublets of the same spin and opposite parity situated far from other similar levels. In this case the parity impurities are well approximated by simple two-state mixing, which simplifies

the analysis and isolates specific components of the PNC-NN interaction. Bearing in mind that for PMDs the ratio $M_{PNC}/\Delta E$ (which estimates roughly the corresponding PNC effect) is usually of the order of 10^{-8} for $\Delta E \geq 1.0$ MeV, we can define a specific enhancement factor: $F=10^8 \times (M_{PNC}/\Delta E) \times f$, where f is the ratio of the decay (formation) amplitude corresponding to the small-lifetime (large-width) level to that of the large-lifetime (small-width) level.

The effects related to the PMD should help to determine the relative strengths of the different components of the PNC nucleon–nucleon (PNC-NN) interaction.[13–16] Owing to the generally small values of most of the terms contributing to the PNC matrix elements, PNC in the low-energy nuclear spectrum should essentially involve the strength of the nucleon–nucleus weak force. As weak interactions do not conserve the isospin, this strength can be characterized by two numbers, relative to the proton and neutron forces, respectively, or, equivalently, to its isovector and isoscalar components. Moreover, the main contribution coming from the isovector part is assumed to be due to the one-pion exchange term (the long-range term), while the main contribution coming from the isoscalar part is assumed to be due to the one ρ-meson exchange term (the short-range term). At present one cannot devise any experiment that would be sensitive to other contributions to the weak hadron–hadron interaction potential. Therefore, in principle two independent experiments should be sufficient for the determination of the above nucleon–nucleus weak forces. They may be those looked at in ^{19}F, whose theoretical analysis[16,24,25] shows that it is dominated by the strength of the proton–nucleus weak force,[23] and in ^{18}F, which is well known to be dominated by the isovector part of this force. The first effect, which is observed experimentally,[18,19] is accounted for by the "best *DDH values*"[13] of the meson–nucleon weak coupling constants. The second one is not, although it is compatible with the largest range of their expectations. Several cases have been proposed theoretically, but only a few of them have been experimentally investigated; only the ^{18}F experiments (average of five investigations[49–53]; Ref. 16) give a reliable upper limit (i.e., $\simeq 10^{-7}$) for the weak pion–nucleon coupling constant. The result is not in contradiction with the predictions of Refs. 13–15, especially if one takes into account more sophisticated recent shell-model calculations,[29,43] which indicate values for the circular polarization much smaller than $\simeq 10^{-4}$. In addition, if one takes into account the analyzing power ($\simeq 2\cdot 10^{-2}$) (Ref. 17) of the Compton polarimeters, this would require a precision $\simeq 1.2\cdot 10^{-5}$ in the counting asymmetry, and it might be very difficult to maintain systematic errors below this limit. Therefore, additional investigations are necessary, especially with independent observables.

This goal was a challenge in the past 15 years. Several pairs of experiments have been proposed in order to separate the isoscalar contributions of the PNC weak force from the isovector ones. Among them we mention the cases presented in Table I.

The above selection could be reasonably due to the fact that the shell-structure problems, for one nucleus or for two adjacent mirror nuclei in selecting the relative weight of the isovector and isoscalar terms entering the structure of the PNC weak force, should not be too different. Unfortunately, the lack of such "*pair*" experimental data does not allow us to extract with high accuracy the isovector and isoscalar components directly from experiment.

Investigating the PNC meson–nucleon vertices within the framework of a chiral effective Lagrangian for π, ρ, and ω meson exchange and treating nucleons as topological solitons, the weak πN coupling constant (h_π) is found[15] to be considerably smaller [$(2.0)\cdot 10^{-8}$] than the standard quark-model results [$(1.3)\cdot 10^{-7}$],[14] both restricting the often used Desplanques, Donoghue, and Holstein (DDH) values[13] significantly. Such a controversy stimulates us to investigate experiments sensitive to h_π with greater interest.

2. NATURE OF THE HADRON–HADRON WEAK INTERACTION THAT VIOLATES THE PARITY-CONSERVATION LAW

In 1957, the same year that PNC was discovered in β and μ decay, Tanner[79] reported the first research concerning parity violation in the hadron–hadron interaction, namely, the parity-forbidden α decay of ^{20}Ne [^{20}Ne ($J^\pi T=1^+0$, $E_x=13.19$ MeV)$\rightarrow ^{16}$O$+\alpha_0$]. This was followed by the Feynman–Gell-Mann[80] universal current–current theory of weak interactions, which predicted, in addition to the known weak processes of β, μ, and hyperon decay, a weak parity-violating interaction between nucleons, which was experimentally established by Lobashev and his co-workers.[66,81]

According to the standard SU(2)⊗U(1) theory of electroweak interactions and quantum chromodynamics (QCD), the nuclear PNC effects arise through weak emission and absorption of the gauge bosons $W^\pm$ and Z^0 by the quarks in the hadrons. Actually, owing to the large masses of the gauge bosons, this elementary weak interaction is of extremely short range. On the other hand, at low energies the nucleons are prevented from coming close together, owing to the hard core in the strong nucleon–nucleon potential. A gauge boson emitted by a quark is subsequently absorbed by a quark belonging to the same nucleon. Therefore, exchange of a gauge boson between distinct nucleons is a highly improbable process. As a result, the nucleon passes into an excited state of quarks, which, at low energies, can be reasonably assumed to be a meson–nucleon state. The meson appears to be emitted by the nucleon through a weak PNC process, with an effective coupling constant which includes all the elementary weak ($h^{(\Delta T)}_{meson}$) and strong ($g^{(\Delta T)}_{meson}$) interactions of the quarks that contributed to the emission. The PNC process in nuclei arises, therefore, through weak PNC emission and absorption of low-mass mesons (π, ρ, and ω) by the nucleons inside the nucleus, neutral scalar mesons being excluded by CP conservation.[16,17,82].

The magnitude of the weak interaction can be estimated, e.g., from the charged weak Hamiltonian:[17]

$$H_W = g^2 \int d^3x_1 d^3x_2 \; j^\mu(x_1) e^{-M_W r_{12}/r_{12}} \; j^\dagger_\mu(x_2). \qquad (1)$$

The mass of the W boson is very large, and the associated length is very short, at the nuclear scale: $M_W \simeq 80$ GeV,

$M_W^{-1} \simeq 2 \cdot 10^{-3}$ fm.[9,10] One can therefore approximate $e^{-M_W r_{12}/r_{12}}$ by a δ function, and Eq. (1) gives

$$H_W = \frac{G}{\sqrt{2}} \int d^3x_1 d^3x_2 \; j^{\mu}(x_1) j_{\mu}^{\dagger}(x_2) \tag{2}$$

with $G = 4\pi\sqrt{2} g^2 / M_W$; thus, the weak coupling constant is of the order of $h \approx g/M_W$.

In the low-energy regime of interest to us, the hadronic weak interaction can be described by a phenomenological current–current Lagrangian[92,93]

$$L = \frac{G_F}{\sqrt{2}} \left(J_C^{\dagger} J_C + 2 \left(\frac{M_W}{M_Z \cos \theta_C} \right)^2 J_N^{\dagger} J_N + \text{H.c.} \right), \tag{3}$$

where J_C and J_N are the charged and neutral currents, respectively, and

$$\frac{G_F}{\sqrt{2}} = \frac{\pi \alpha}{2 M_W^2 \sin^2 \theta_W}, \tag{4}$$

in which $\alpha = e^2/4\pi$ is the fine-structure constant, M_W and M_Z are the masses of the heavy $W^{\pm}$ and Z bosons, respectively, and θ_C and θ_W are the Cabibbo and Weinberg angles, respectively.

The charged current J_C has two components:

$$J_C = \cos \theta_C \, J_W^0 + \sin \theta_C \, J_W^1. \tag{5}$$

The superscripts 0 and 1 stand for the isospin transfer (ΔT). The neutral current J_Z also has two components, J_Z^0 and J_Z^1, which transform as $\Delta T = 0$ and 1, respectively. All the components of the charged and neutral currents, except the J_W^1 component of the charged current, transform as $\Delta S = 0$, where S is the strangeness quantum number. The component J_W^1 is not very important because it is suppressed by $\tan^2 \theta_C$.[11,12] On the other hand, the $\Delta T = 1$ neutral-current contribution is not suppressed. Therefore, on these simple grounds, we expect the neutral current to dominate the $\Delta T = 1$ PNC nucleon–nucleon interaction. However, the strong interaction can significantly alter the PNC matrix elements, so that this qualitative isospin argument may not always be valid.

The earliest experiments[81] have used the knowledge of low-energy nuclear interactions and looked for the very small ($\approx 10^{-6}$) parity mixing of levels at the magnitude expected on the basis of previous studies in the language of meson exchange.[94]

It is well known that the parity-conserving (PC) nucleon–nucleon force can be described reasonably well in terms of a coherent superposition of diagrams for meson exchange. In a similar fashion one generally represents the PNC-NN potential in terms of a sum of diagrams involving exchange of a single meson between pairs of nucleons. There is an important difference in this case, however, in that one meson–nucleon vertex is weak and one is strong. Insofar as CP violation is negligible,[82] the PNC–NN potential is determined by π, ρ, and ω exchange.

Since the strong coupling constants are empirically known, one finds a form of the PNC-NN potential in terms of seven weak coupling constants ($h_{\text{meson}}^{\Delta T}$). All the physics of W and Z exchange between the quarks of the nucleons and mesons is hidden inside these weak coupling constants.[13–15,95] The shape of this PNC interaction potential is determined by the nature of the exchanged meson.

Coming back to the approaches to get a handle on the weak coupling constants ($h_{\text{meson}}^{\Delta T}$), some comments could be in order here.

Within the standard model, one needs to calculate the weak meson–nucleon vertices. Only a few calculations based on the quark model (Refs. 13, 14, 58, 59, 61, and 62) exist. In Refs. 13 and 14 the authors employed an SU(6) quark model to calculate six weak meson–nucleon coupling constants ($h_{\text{meson}}^{\Delta T}$): $h_{\pi}^{(1)}, h_{\rho}^{(0)}, h_{\rho}^{(1)}, h_{\rho}^{(2)}, h_{\omega}^{(0)}, h_{\omega}^{(1)}$. These calculations start from the observation that there are essentially three types of diagrams, which can be categorized as factorization, quark-model, and sum-rule contributions. Renormalization-group techniques and baryon wave functions based on phenomenological models are needed to evaluate them. This introduces a variety of uncertainties ($\cong 300\%$), which lead DDH in Ref. 13 to introduce a "reasonable range" for the values of the weak meson–nucleon coupling constants. In particular, the weak pion–nucleon coupling constant (h_{π}) is very sensitive to these uncertainties; for instance, the values of h_{π} differ by a factor of 3 in Refs. 13 and 14, whereas $h_{\rho(\omega)}$ are more stable. In addition, recent QCD sum-rule applications lead[59] to the estimate $h_{\pi}^{(1)} \approx (3.0) \cdot 10^{-8}$. QCD sum rules have been shown to be able to reproduce known properties of the nucleon (e.g., μ_p, μ_n, g_A) and of other hadrons.[60] However, they have rarely (if ever) been used to predict unknown properties, such as the value of $h_{\pi}^{(1)}$.

By using a nonlinear chiral effective Lagrangian which includes π, ρ, and ω mesons and treating nucleons as topological solitons, Kaiser and Meisner[15] obtained values for the strong and weak meson–nucleon coupling constants slightly different from the results in Refs. 13 and 14. The largest discrepancy concerns the weak meson–nucleon coupling constant h_{π}, which is 20 times smaller than the "best value" given in Ref. 13. Moreover, Kaiser and Meisner[15] obtained in addition the seventh weak meson–nucleon coupling constant $(h^{(1)})_{\rho'}$, with a quite large value, giving a comparable contribution to the pion term in some PNC processes (see, for example, Refs. 46 and 47). For comparison, we inserted in the calculations of the PNC matrix element mentioned above the coupling constants of the weak meson–nucleon vertices, h_{π}, h_{ρ}, and h_{ω}, calculated within different models of the weak interactions and summarized in Tables II and III. The first column of Table II contains $h_m^{(\Delta T)}$ obtained by Kaiser and Meisner (KM),[15] using their model parameters as follows: the pion decay constant $f_{\pi} = 93$ MeV, the "gauge" coupling constant $g_{\rho\pi\pi} = 6$, the pion mass $m_{\pi} = 138$ MeV, and three pseudoscalar–vector coupling constants (see Table I of Ref. 15; Table II of the same reference includes the strong coupling constants as well). The second column contains the often used Desplanques, Donoghue, and Holstein (DDH)[13] "best" values obtained within a quark plus Weinberg–Salam model. In the third column the fitted (from experiments) values of $h_m^{(\Delta T)}$ given by Adelberger and Haxton[16] are listed. In the last column the values obtained by

Dubovik and Zenkin (DZ)[14] within a more sophisticated quark plus Weinberg–Salam [SU(2)⊗U(1)⊗SU(3)$_C$] model are included. We consider these values as more "reasonable," taking into account the fact that they are sustained by comparison with the experimental data given in the comprehensive review of Adelberger and Haxton (AH).[16]

The approach of Kaiser and Meissner[15] is based on the soliton picture of the baryons, which takes into account important nonperturbative effects of QCD at low energies. The fact that the baryons may emerge as solitons from an effective meson Lagrangian with its intriguing connections to the chiral anomalies was suggested by Skyrme,[83] and it has met with remarkable success in a variety of applications.[85–89] The Skyrme model deals with an effective theory of mesons, specifically with pions, and how to obtain baryons and their interactions in such a theory. The broad interest in this model recently in the theory of strongly interacting particles is due to speculations that effective theories of mesons may provide a link between QCD and the familiar picture of baryons interacting via meson exchange. This last picture has proven very useful in the past for energies up to the GeV region, because in this "low" energy domain QCD becomes forbiddingly difficult, owing to the rising coupling constants, thus posing a major obstacle to a satisfactory description of the dynamical behavior of the elementary quark and gluon fields of QCD at the relevant large distances. Some nonlinear field theories may have special solutions (solitons), and this led to Witten's suggestion[84] that baryons may be regarded as soliton solutions of the effective meson theory without any further reference to their quark content. This approach includes two distinct aspects: 1) the relation of the form of the effective nonlinear meson theory to QCD; 2) the treatment of the structure of the baryons, which results from the effective Lagrangians, their interactions among themselves, and their interactions with antibaryons or with mesons. Fortunately, the second aspect can be considered quite independently of an eventual answer to the first question, which is quite difficult at the moment, because the underlying symmetries and the restriction to low energies impose limitations on the possible forms of the effective Lagrangians. Most of the results, it is assumed, will not depend on the specific details of the chosen Lagrangian at all, but will simply reflect symmetries and the fact that baryons are considered as soliton configurations in the basic meson field theory. Of course, not knowing the true effective theory, we cannot expect quantitative agreement with the experimental data; however, if the whole concept is to make sense, we should certainly expect that essential features of baryon structure and interactions should at least be qualitatively reproduced. In addition to the abovementioned sources of uncertainties in calculating the weak meson–nucleon coupling constants ($h^{(\Delta T)}_{\text{meson}}$), the chiral soliton treatment of the problem, in spite of its nonperturbative aspect, contains other shortcomings such as a simplified quantization procedure, leading to higher masses and strong coupling constants for the nucleons, and restrictions to the two-flavor sector, the three-flavor sector being more appropriate because of possible strangeness admixtures in the proton wave functions.

Such a controversy greatly stimulates the investigation of possible experiments sensitive to the value of $h^{(1)}_{\pi}$.

The usual PNC-NN potential[29] has the form

$$H_{\text{PNC}}=\sum_{\Delta T,s=\pi,\rho,\omega} V_s^{\text{PNC}}(\Delta T)=\sum_{\Delta T,k,s=\pi,\rho,\omega} F_{k,s}^{\Delta T} f_{k,s}^{\Delta T}, \tag{6}$$

where the terms $V_s^{\text{PNC}}(\Delta T)$ are different meson contributions to the total PNC-NN potential (H_{PNC}):

$$\begin{aligned}
V_{\pi}^{\text{PNC}}(\Delta T=1)&=\frac{1}{2\sqrt{2}}\, g_{\pi} h_{\pi}^{(1)} f_{0,\pi}^{(1)},\\
V_{\rho}^{\text{PNC}}(\Delta T=1)&=-\tfrac{1}{2}\, g_{\rho} h_{\rho}^{(1)}[f_{1,\rho}^{(1)}-f_{3,\rho}^{(1)}+(1+\mu_v) f_{2,\rho}^{(1)}],\\
V_{\omega}^{\text{PNC}}(\Delta T=1)&=-\tfrac{1}{2}\, g_{\omega} h_{\omega}^{(1)}[f_{1,\omega}^{(1)}+f_{3,\omega}^{(1)}+(1+\mu_s) f_{2,\omega}^{(1)}],\\
V_{\rho'}^{\text{PNC}}(\Delta T=1)&=-\tfrac{1}{2}\, g_{\rho} h_{\rho'}^{(1)} f_{0,\rho}^{(1)},\\
V_{\rho}^{\text{PNC}}(\Delta T=0)&=-g_{\rho} h_{\rho}^{(0)}((1+\mu_v)+f_{4\rho}^{(0)}+f_{5\rho}^{(0)}),\\
V_{\omega}^{\text{PNC}}(\Delta T=0)&=-g_{\omega} h_{\omega}^{(0)}((1+\mu_s) f_{6\omega}^{(0)}+f_{7\omega}^{(0)}),\\
V_{\rho}^{\text{PNC}}(\Delta T=2)&=-\frac{1}{2\sqrt{6}}\, g_{\rho} h_{\rho}^{(2)}((1+\mu_v) f_{8\rho}^{(2)}+f_{9\rho}^{(2)}),
\end{aligned} \tag{7}$$

in which

$$\begin{aligned}
f_{0,s}^{(1)}&=\frac{1}{2M_N}\, i[\vec{\tau}_1\times\vec{\tau}_2]_z(\vec{\sigma}_1+\vec{\sigma}_2)\cdot\vec{u}(\vec{r},m_s),\\
f_{1,s}^{(1)}&=\frac{1}{2M_N}\,(\tau_{1_z}+\tau_{2_z})(\vec{\sigma}_1-\vec{\sigma}_2)\cdot\vec{v}(\vec{r},m_s),\\
f_{2,s}^{(1)}&=\frac{1}{2M_N}\,(\tau_{1_z}+\tau_{2_z}) i(\vec{\sigma}_1\times\vec{\sigma}_2)\cdot\vec{u}(\vec{r},m_s),\\
f_{3,s}^{(1)}&=\frac{1}{2M_N}\,(\tau_{1_z}-\tau_{2_z})(\vec{\sigma}_1+\vec{\sigma}_2)\cdot\vec{v}(\vec{r},m_s),\\
f_{4,s}^{(0)}&=\frac{1}{2M_N}\,(\vec{\tau}_1\cdot\vec{\tau}_2) i[\sigma_1\times\sigma_2]\cdot\vec{u}(\vec{r},m_s),\\
f_{5,s}^{(0)}&=\frac{1}{2M_N}\,(\vec{\tau}_1\cdot\vec{\tau}_2)(\vec{\sigma}_1-\vec{\sigma}_2)\cdot\vec{v}(\vec{r},m_s),\\
f_{6,s}^{(0)}&=\frac{1}{2M_N}\, i[\vec{\sigma}_1\times\vec{\sigma}_2]\cdot\vec{u}(\vec{r},m_s),\\
f_{7,s}^{(0)}&=\frac{1}{2M_N}\,(\vec{\sigma}_1-\vec{\sigma}_2)\cdot\vec{v}(\vec{r},m_s),\\
f_{8,s}^{(2)}&=\frac{1}{2M_N}\,[3\tau(1)_z\tau(2)_z-\vec{\tau}(1)\cdot\vec{\tau}(2)]\cdot i[\vec{\sigma}(1)\\
&\quad\times\vec{\sigma}(2)]\cdot\vec{u}(\vec{r},m_s),\\
f_{9,s}^{(2)}&=\frac{1}{2M_N}\,[3\tau(1)_z\tau(2)_z-\vec{\tau}(1)\cdot\vec{\tau}(2)]\cdot[\vec{\sigma}(1)\\
&\quad-\vec{\sigma}(2)]\cdot\vec{v}(\vec{r},m_s),
\end{aligned} \tag{8}$$

with

$$\vec{u}(\vec{r},m_s)=\left[(\vec{p}_1-\vec{p}_2),\frac{1}{4\pi r}\exp(-m_s r)\right]_-, \quad (9)$$

$$\vec{v}(\vec{r},m_s)=\left\{(\vec{p}_1-\vec{p}_2),\frac{1}{4\pi r}\exp(-m_s r)\right\}_+. \quad (10)$$

Here

$$g_\pi=13.45,\quad g_\rho=2.79,\quad g_\omega=8.37,\quad \vec{r}=\vec{r}_1-\vec{r}_2,$$
$$\mu_v=3.7,\quad \mu_s=-0.12.$$

Recently, it was proposed[96] to consider a new parity-violating mechanism, specific for nucleons bound in the nucleus, and it was shown that this mechanism generates a new term in $H_{\rm PNC}$, which is sometimes of the same order as the above terms. This mechanism consists of weak emission and absorption of mesons by a single nucleon in the presence of the strong nuclear field. This PNC process is forbidden for a free nucleon by time-reversal invariance; it can occur, however, for a nucleon interacting with a nuclear field. A similar situation occurs in quantum electrodynamics, where the interaction of a bound electron with the radiation field leads to a modification of the Coulomb potential, responsible for the well known Lamb shift.[97]

The form of this single-particle PNC interaction potential depends on the choice of the relativistic potential $V^\mu\cdot S$ (see Ref. 98),

$$S=(\tfrac{1}{2}U_0-2M^2r_0^2U_{ls})\cdot f(r);$$

$$V^0=(\tfrac{1}{2}U_0+2M^2r_0^2U_{ls})\cdot f(r);\quad V^i=0;\quad i=1,2,3, \quad (11)$$

describing the external field, and not on the nature of the exchanged meson. Its expression is[96]

$$V_{\rm PNC}^{\rm CM}=\frac{(\alpha T)^s}{M^2}\left(\frac{U_0}{4M}+U_{ls}Mr_0^2\right)\{\vec{\sigma}\cdot\vec{p},\Delta f(r)\}. \quad (12)$$

Here $\vec{p}$ denotes the momentum operator of the nucleon. The (αT) coupling constants depend on $h_{\rm meson}^{(\Delta T)}$: $h_\pi^{(1)},h_\rho^{(o)},h_\rho^{(1)}$, $h_\rho^{(2)},h_{\rho'}^{(1)},h_\omega^{(0)},h_\omega^{(1)}$ and sometimes on the τ_3 component of the isospin. This new PNC term (12) should be added to the PNC matrix elements with no isospin change and, hence, it does not contribute to the isovector PNC matrix elements. A crude estimation of the magnitude of this new contribution to $H_{\rm PNC}$, e.g., from the term containing $h_\rho^{(1)}$, is given as follows. Denoting the ratio of $M_{\rm PNC}^{\rm CM}(h_\rho^{(0)})$ and $M_{\rm PNC}^{\rm DDH}(h_\rho^{(0)})$ by R, Caprini and Micu[96] found $R=24/(9\gamma A^{2/3})$, where γ is an overall reduction factor due to short-range correlations; this ratio, for instance, in the case of ^{14}N PMD1, is $\simeq 1/4$.

In view of these results, it may be of interest to reconsider meson exchanges other than those permitted by Barton's theorem.[82]

3. SHELL-MODEL PREDICTIONS FOR PARITY-MIXING MATRIX ELEMENTS

The calculation of PNC effects in the nucleus is usually divided into four parts. The first part belongs to elementary-particle physics. In this part the weak $(h_{m-N}^{(\Delta T)})$ and strong (g_{m-N}) meson–nucleon coupling constants are calculated starting from the quark structure of the hadrons and their elementary interactions[13,14] or by applying effective theories of mesons and baryons[85–89] such as the soliton picture of the nucleon,[15] which takes into account important nonperturbative effects of QCD at low energies. These coupling constants enter as input in the second part of the analysis, where the quantum fluctuations consisting of meson emission and absorption in the nucleus are explored and their effects are expressed as an equivalent nonrelativistic PNC nuclear Hamiltonian ($H_{\rm PNC}$). The form of the PNC interaction potential ($H_{\rm PNC}$) is determined by the nature of the exchanged meson, while the information related to the weak-interaction vertex, the most poorly known part, is contained in seven coupling constants $h_{\rm meson}^{(\Delta T)}$: $h_\pi^{(1)},h_\rho^{(0)},h_\rho^{(1)},h_\rho^{(2)},h_{\rho'}^{(1)},h_\omega^{(0)},h_\omega^{(1)}$. In the third part we need nuclear-matter techniques. To compute the PNC matrix elements ($M_{\rm PNC}$) of $H_{\rm PNC}$ between nuclear wave functions we need to evaluate the short-range correlations (SRC) (Refs. 90, 91, 99, and 100), which describe the effect of the distortion of the relative two-nucleon wave functions at small distances due to the strong repulsive core in the nuclear interaction. The repulsion punches a hole in the relative two-nucleon wave functions near the origin, and this has strong effects on two-body observables, e.g., those generated by $H_{\rm PNC}$, which is of very short range (less than 1.5 fm, while the core radius is $\simeq$0.5 fm). The SRC act as a renormalization of $H_{\rm PNC}$.[20] The matrix elements of this "renormalized" potential between nuclear wave functions are finally evaluated (the fourth part), in order to obtain predictions for measurable quantities, such as rates of forbidden transitions (pseudoscalar observables: PNC asymmetries, analyzing powers, and circular polarizations; or, directly, the PNC decay rates, e.g., the PNC α-decay rates,[16,17,22,44] optical rotation parameters,[21] etc.) In particular, the OXBASH shell-model code in the Michigan State University version (Refs. 24, 25, 57, 63, and 111–118) is situated along the fourth step of the above-mentioned program.

In order to determine the range and amplitude of the PNC observables around the excitation energy of the PMDs, we have made a shell-model estimate of the PNC matrix element, using the OXBASH code, which includes different model spaces and different residual effective two-nucleon interactions:

$$M_{\rm PNC}=\langle J^-{}^\pi T,E_x(\text{MeV})|H_{\rm PNC}|J^\pi T',E_x'(\text{MeV})\rangle$$
$$=\sum_{\Delta T,k,s=\pi,\rho,\omega}F_{k,s}^{(\Delta T)}M_{\Delta T,k,s}^{\rm PNC}, \quad (13)$$

where

$$M_{\Delta T,k,s}^{\rm PNC}=\langle J^-{}^\pi T,E_x(\text{MeV})|f_{k,s}^{(\Delta T)}|J^\pi T',E_x'(\text{MeV})\rangle \quad (14)$$

are different [see Eq. (8)] nuclear-structure matrix elements (in MeV).

To obtain the effective two-body interactions (ETBI) we can use, e.g., the G-matrix method (Refs. 73–75 and 99–103) by solving the generalized Bethe–Goldstone[99] or Bethe–Faddeev[100] equations. The method is iterative:[101]

1) first, a complete set of single-particle (s.p.) states is chosen (in the OXBASH code, s.p. oscillator states are chosen);

2) the reaction G-matrix is then calculated, and a first iterated ETBI is obtained;

3) the Hartree-Fock (HF) equation with this ETBI is solved, to yield a first iteration of the occupied s.p. energies and wave functions;

4) the generalized Bethe-Goldstone and Bethe-Faddeev equations are solved in order to establish the unoccupied-state potential;

5) the Schrödinger equation for the unoccupied s.p. energies and wave functions is solved;

6) the unoccupied s.p. basis is orthogonalized to the occupied s.p. states found at step 3, to give the first iteration for the unoccupied s.p. states.

Having in this way a complete set of first-iterated s.p. states, we repeat a second cycle starting with step 2. After a number of iterations, depending on the quality of the first-chosen s.p. basis and the G matrix, we obtain the last-iterated s.p. basis and the ETBI.

The ETBI obtained in this way is diagonalized in the last-iterated s.p. basis (m scheme) or in a more sophisticated basis obtained by different coupling and projection procedures.[113]

The ETBI and the s.p.-basis parameters can also be extracted from experimental data.

Our calculations use both procedures.

In these calculations the ZBM, PSD, D3F7, and SDPFW model spaces have been used.

Let us denote the shell-model orbits as follows:

orbits:	$1s_{1/2}$	$1p_{3/2}$	$1p_{1/2}$	$1d_{5/2}$	$1d_{3/2}$	$2s_{1/2}$	$1f_{7/2}$	$2p_{3/2}$	$2p_{1/2}$
number:	1	2	3	4	5	6	7	8	9

In these calculations the ZBM, PSD, D3F7, and SDPF model spaces have been used:

model space	filled orbits	valence orbits
ZBM	1,2	3,4,6
PSD	1	2,3,4,5,6
D3F7	1,2,3,4	5,7
SDPF	1,2,3	4,5,6,7,8,9

The abbreviation ZBM should be understood as the Zucker–Buck–McGrory model space.[76] In Ref. 76 the single-particle energies were fitted to the values obtained from experiment, and the two-body matrix elements (TBME) were identified with Kuo and Brown G-matrix elements (the F interaction is abbreviated as ZBMI).[25,71,72] Within the ZBMI we are dealing with the same model space as above. A fitting procedure for two single-particle energies and for 30 TBME in the mass region $A=13-17$ was performed (the Z interaction).[25,76,77] REWIL makes a 33-parameter fit to the spectra in the mass region $A=13-22$.[104] In the ZWM and ZBMO the two-body matrix elements are calculated by using a Hamada–Johnston G matrix[112] and the Oxford Avila–Aguirre–Brown[63] interactions, respectively. The center-of-mass spurious components in the wave functions have been eliminated according to the prescription given in Ref. 118.

Within the PSDMK the PSD model space is used, and the interactions are as follows: for the P space, the Cohen–Kurath interaction;[105] for the SD space, the Preedom–Wildenthal interaction;[106] for the coupling matrix elements between the P and SD spaces, the Millener–Kurath interaction,[107] which is very close to the G-matrix one. PSDMWK uses the same PSD model space, and the only change as compared with PSDMK is that in the SD space the Wildenthal[114] interaction is used.

Within the D3F7 model space the single-particle energies and the two-body matrix elements were fitted. In the calculations we denoted the different interactions as follows: HW stands for the Hsieh–Wildenthal interaction,[63] WO and W4 for other Wildenthal interactions as used in Refs. 115 and 114, respectively, and FEPQ for the Federman–Pittel interaction.[116]

In the SDPF calculations of the natural-parity states it was sufficient to consider the restriction to the sd major shell.

In most of the cases there are two types of contributions to the PNC matrix element: one coming from two-body transition densities (TBTD), if all four orbitals entering into the two-body matrix elements (TBME) are in the valence space,[25] and another from the one-body transition densities (OBTD), if two orbitals are in the core. For instance, in the case of ^{16}O PMD1, the only contribution to the latter comes from the following matrix element:

$$\langle (1s_{1/2})^4(1p_{3/2})^8 2s_{1/2} \| H_{\rm PNC} \| (1s_{1/2})^4(1p_{3/2})^8 1p_{1/2} \rangle, \qquad (15)$$

which turns out to be the dominant one in all the cases described above.

3.1. Short-range correlations

Since all the components[13,16] of $H_{\rm PNC}$ are short-range two-body operators, and bearing in mind that the behavior of the shell-model wave functions at short relative NN distances is wrong, it is necessary to use shell-model wave functions including short-range correlations (SRC) to calculate correctly their matrix elements. The correlations were included by multiplying the harmonic-oscillator wave functions (with $\hbar\omega=41/A^{1/3}$ MeV) by the Jastrow factor:

$$1-\exp(-ar^2)(1-br^2), \quad a=1.1 \text{ fm}^{-2},$$
$$b=0.68 \text{ fm}^{-2}, \qquad (16)$$

given by Miller and Spencer.[65] This choice is consistent with results obtained by using more elaborate treatments of SRC such as the generalized Bethe–Goldstone approach[20,66,67] and should correspond roughly to an NN interaction close to the Reid soft-core model for the $^1S_0$ and $^3P_0$ components. Comparison with more recent models of the NN strong interactions[68] indicates that the Miller and Spencer approach (16) overestimates the effect of the short-range repulsion. From inspection of the $^3S_1$ component of the deuteron wave function, one thus expects that the correlation function does not vanish at the origin. With the same asymptotic normalization as in (16), it would be close to 0.1 for the Paris model[69] and 0.5 for the Bonn model.[68] Moreover, the correlation function (16) neglects the effect of the tensor force, which admixes to the $^3S_1$ state a $^3D_1$ component, which also

has a short-range character. This effect is large and, depending on the transition amplitude, is constructive or destructive.[137] In the case of the π-exchange contribution, dominated by the $^3P_1-^3S_1(+^3D_1)$ transition, it compensates a large part of the short-range repulsion.[137] On the other hand, in the case of the isoscalar ρ-exchange contribution, *a priori* dominated by the $^1P_1-^3S_1(+^3D_1)$ transition, it provides further suppression.

The above improvements should be incorporated in definitive predictions. We will not do this and will stick to (16). First, there is no point in playing with different models of short-range correlations. Second, there are other possible improvements due, for instance, to the part of the 2π exchange contribution not included in the ρ, to vertex form factors, to heavier-meson exchanges, etc. Furthermore, the corresponding uncertainties will add to those in the PNC coupling constants themselves. We feel that it is more important to make predictions that can be compared with other ones than to multiply them by looking at modifications of rather minor relevance at the present time. The essential point is that the PNC potential given by (6) can account independently for the various contributions expected to dominate at low energy and which are due to the PNC-NN transition amplitudes $^1S_0-^1P_0$ (three amplitudes: pp, nn, and pn, or $\Delta T=0$, 1, and 2), $^3S_1-^3P_1$ (pn, $\Delta T=0$), and $^3S_1-^3P_1$ (pn, $\Delta T=1$). A few clues as to the relevance of these amplitudes will be given when discussing the results.

By including SRC the PNC pion-exchange matrix element decreases by 40–50 without including SRC, while the $\rho(\omega)$-exchange matrix elements also decrease by a factor of 1/3–1/7.

3.2. The Lanczos technique

The OXBASH code includes a powerful algorithm based on the work of Lanczos.[108,109] Some of the techniques that we use might be equally effective for some heavy nuclear regions and high spin, particularly when the spin is close to the limiting value in the chosen shell-model space.

The basic tool, the Lanczos algorithm, allows one to find the extremum (lowest and highest) eigenvalues and associated eigenvectors of a very large matrix iteratively. With standard workstations, matrices of dimension $\simeq 10^6$ by 10^6 can be treated in this way. In contrast, standard methods for fully diagonalizing matrices are usually limited to $\simeq 10^3$ by 10^3 (Ref. 110). An even more powerful aspect of this algorithm, due to its connections with the method of moments, is that it can be used to generate inclusive response functions and Green's functions iteratively. Thus, the Lanczos algorithm has proven useful in a wide variety of problems, including the nuclear shell model, atomic and molecular structure, spin lattice problems in condensed-matter physics, and Hamiltonian lattice gauge theory. In what follows we sketch the algorithm, especially for nuclear-structure applications.

Consider a Hamiltonian H, defined over a finite Hilbert space of dimension N, and a starting normalized vector $|\psi_1\rangle$ in that space. We begin to construct a basis for representing

$$H=\sum_{mn} |\psi_n\rangle H_{mn}\langle\psi_m| \tag{17}$$

by

$$H|\psi_1\rangle=\alpha_1|\psi_1\rangle+\beta_1|\psi_2\rangle, \tag{18}$$

where $|\psi_2\rangle$ is a normalized vector representing that part of $H|\psi_1\rangle$ orthogonal to $|\psi_1\rangle$, i.e.,

$$\beta_1|\psi_2\rangle=\sum_{n\neq 1} H_{1n}|\psi_n\rangle, \quad \alpha_1=H_{11}. \tag{19}$$

Proceeding, we obtain

$$H|\psi_2\rangle=\beta_1|\psi_1\rangle+\alpha_2|\psi_2\rangle+\beta_2|\psi_3\rangle, \tag{20}$$

$$H|\psi_3\rangle=\beta_2|\psi_2\rangle+\alpha_3|\psi_3\rangle+\beta_3|\psi_4\rangle, \tag{21}$$

and so on. Note that the term $\beta_1|\psi_1\rangle$ must appear in the first line above because H is Hermitian. Note also that $|\psi_1\rangle$ does not appear in the second line above because everything that connects to $H|\psi_1\rangle$ other than $|\psi_1\rangle$ is defined as $|\psi_2\rangle$. Similarly, $H|\psi_4\rangle$ will contain nothing proportional to $|\psi_1\rangle$ or $|\psi_2\rangle$. Thus, H has been cast in a tridiagonal form:

$$H=\begin{pmatrix} \alpha_1 & \beta_1 & 0 & 0 & \dots \\ \beta_1 & \alpha_2 & \beta_2 & 0 & \dots \\ 0 & \beta_2 & \alpha_3 & \beta_3 & \dots \\ 0 & 0 & \beta_3 & \alpha_4 & \dots \\ \dots & \dots & \dots & \dots & \dots \end{pmatrix}. \tag{22}$$

As an example, within the ZBM[76] model space for the $|\psi_1\rangle$ starting vector one can use one of the vectors

$$\left|\left\{\left[(1d_{5/2})^{n_1}_{I_1T_1}\cdot(2s_{1/2})^{n_2}_{I_2T_2}\right]^{(n_1+n_2)}_{I_{12}T_{12}}\cdot(1p_{1/2})^{n_3}_{I_3T_3}\right\}^{(\Sigma_{i=1}^3 n_i)=4}_{IT}\right\rangle \tag{23}$$

constructed in an oscillator single-particle basis.

If this procedure is continued for N steps, the full H would then be in tridiagonal form. However, the power of the algorithm derives from the information in the tridiagonal Lanczos matrix when the procedure is truncated after n iterations, with $n\ll N$. If Ψ_{E_i} $(i=1,\dots,N)$ are the exact eigenfunctions of H, then

$$\langle\psi_1|H^\lambda|\psi_1\rangle=\sum_{i=1}^{N}|\langle\psi_1|\Psi_{E_i}\rangle|^2E_i^\lambda\equiv\sum_{i=1}^{N}f(E_i)E_i^\lambda. \tag{24}$$

The distribution $f(E_i)$ $(i=1,\dots,N)$ can be thought of a set of N weights f and measures E_i (the eigenvalues) characterizing the distribution of $|\psi_1\rangle$ in energy, i.e., the f's determine a complete set of moments. The truncated Lanczos matrix, when diagonalized, provides the information needed to construct a distribution $g(\tilde{E}_i)$ $(i=1,\dots,n)$, with $\tilde{E}_i\simeq E_i$, which has the same $2n+1$ lowest moments in E as the exact distribution $f(E_i)$ $(i=1,\dots,N)$. In other words, the Lanczos algorithm provides, at each iteration, a solution to the classical moment problem.[109]

4. ASYMMETRIES IN RESONANCE ELASTIC SCATTERING AND NUCLEAR REACTIONS

As a rule, in studying nuclear collisions induced by polarized projectiles that populate a PMD occurring in the compound-nucleus excitation spectrum,[64] the largest magnitude of the PNC effects can be observed,[31–33,56] for a projec-

tile energy around the member of the PMD having the smallest (Γ_c^{small}) partial width (*a narrow resonance*).

In the vicinity of this narrow resonance the PNC analyzing powers [A_L and A_b (Refs. 34, 35, 37, 41, 42, and 54) or alternatively the index $L(b)$, found as $z(x)$ in other studies] have the following simple expression:

$$A_{L(b)}=D_{L(b)}\frac{1}{2}\Gamma^{\text{small}}\left(E-E^{\text{small}}+\frac{i}{2}\Gamma^{\text{small}}\right)^{-1}\times\exp(i(\phi_{L(b)}+\phi_{\text{PNC}})), \quad (25)$$

where

$$D_{L(b)}=2\frac{|M_{\text{PNC}}|}{\left|\left(E-E^{\text{large}}+\frac{i}{2}\Gamma^{\text{large}}\right)\right|}\sqrt{\frac{\Gamma_c^{\text{large}}}{\Gamma_c^{\text{small}}}}|C_{L(b)}| \quad (26)$$

and

$$C_{L(b)}=|C_{L(b)}|e^{(i\phi_{\text{PC}}^{L(b)})}=\frac{\left|\left(E-E^{\text{large}}+\frac{i}{2}\Gamma^{\text{large}}\right)\right|}{\sqrt{\Gamma^{\text{large}}\Gamma^{\text{small}}}}. \quad (27)$$

The quantity

$$\frac{\Sigma_l P_l^{(\kappa)}(\cos\theta)[\Sigma_n c_n^l(L(b))iC(\theta)\tilde{t}_n^*+\Sigma_{mn}b_{mn}^l(L(b))(\tilde{t}_m t_n^*+\tilde{t}_m^* t_n)]}{\Sigma_l P_l(\cos\theta)\Sigma_{mn}a_{mn}^l t_m t_n^*}$$

is a function of the PC transition matrix elements only [for L: $\kappa=0$; for b: $\kappa=1$; and, e.g., for the proton channel (p) we use the notation $\tilde{t}_n=T^{\text{PC}}_{pls,pl_1s_1}]$, $\exp(i(\xi_{pls}-\xi_{pl's'}))$. The coefficients $a_{mn}^{(l)}(L(b))$, $b_{mn}^{(l)}(L(b))$, and $c_n^{(l)}(L(b))$ are simple specific values of the geometrical coefficients for the case that we are investigating (Refs: 34, 35, 37, 41, 42, 54, and 55).

The largest energy anomaly ($\Delta A_{L(b)}$), i.e., the distance between the minimum and the maximum of the PNC analyzing powers of the excitation function in the vicinity of the narrow resonance level, is equal to the quantity $D_{L(b)}$ defined above and does not depend on the PNC matrix-element phase ϕ_{PNC} or the PC-quantity phase $\phi_{L(b)}$:[34]

$$D_{L(b)}=D_{L(b)}^0\left|\sum_{\Delta T,s=\pi,\rho,\omega}V_s^{\text{PNC}}(\Delta T)\right| =D_{L(b)}^0\left|\sum_{\Delta T,k,s}F_{k,s}^{(\Delta T)}M_{k,s}^{(\Delta T)}\right|, \quad (28)$$

where $V_s^{\text{PNC}}(\Delta T)$ (in eV) are different meson contributions to the total PNC shell-model matrix element. The $F_{k,s}$ in units of 10^{-6} are given in Table III (see also Table II of Ref. 23). The $M_{k,s}$ are nuclear-structure matrix elements in units of MeV.

The quantity $D_{L(b)}^{(0)}$ (in eV^{-1}) is given by

$$D_{L(b)}^{(0)}=2\left(E-E^{\text{large}}+\frac{i}{2}\Gamma^{\text{large}}\right)^{-1}\sqrt{\frac{\Gamma_p^{\text{large}}}{\Gamma_p^{\text{small}}}}|C_{L(b)}|. \quad (29)$$

4.1. Parity mixing in ^{14}N

In the excitation spectrum[64] of the ^{14}N nucleus there are two PMDs lying at 8.7 MeV and 9.3 MeV excitation energy (see Table I).

The difference between the two PMDs is that PMD1 is essentially of the isoscalar type, while PMD2 is of the isovector type; hence, we have an interesting case for seeking neutral currents in the structure of the weak hadron–hadron interaction.

There has been only one experiment on PNC effects in the ^{14}N nucleus. In the following we try to explain this Seattle–Madison[56] experiment on the PNC effect around the first PMD in ^{14}N, investigated via $^{13}\text{C}(\vec{\text{p}},\text{p})^{13}\text{C}$ resonance scattering. The only possible measured quantity was the longitudinal analyzing power. The experimental apparatus was developed with symmetry and stability as major design considerations. The maximum count rate attainable for this experiment was governed by the 3.8-keV width of the 0^+1 resonance, since the optimum target thickness is of that order and the maximum current on the target was less than 1 μA. The experiment could be performed by counting the scattered protons individually (expected rates less than 1 MHz). Since the elastic scattering is the only open particle decay channel, the detector resolution was sacrificed for speed. Thin plastic scintillators mounted on 5.1-cm PMTs were used. The relevant features of the detectors are: ~10 nsec pulse width, ~25–30% resolution, a stiff base current to gain stability, robustness toward radiation damage, and large solid angle. There was a fourfold (left–right, up–down) detection geometry with eight detectors azimuthally symmetric about the beam axis, four at $\theta_1=35°$ and four at $\theta_2=155°$. The maximum PNC signal was expected to be the difference $A_L(\theta_2)-A_L(\theta_1)=A_L(b-f)$ (the back–front PNC signal). In such a detection scheme there should be small systematic asymmetries due to position and angle modulations that may be correlated with the beam helicity reversal. The back–front PNC signal gives a self-normalizing system and desensitizes the detector to small target-thickness variations. A target rastering device is used in order to desensitize the detectors to the target irregularities. The long-term correction capabilities, for a typical two-week run, lead to the fact that the transverse asymmetries are kept to a level of $\bar{P}_T A_T<2\cdot10^{-5}$. Because of the energy modulations due to the beam helicity reversal, the measured sensitivity was $\delta A_L(b-f)/\delta E=9\cdot10^{-5}/\text{eV}$; a statistical accuracy $\Delta E=0.2$

TABLE I. Several studied parity-mixed doublets.[30] Here E_i and Γ_i are the excitation energies and total widths of the PMD levels, f is the "small" enhancement factor due to the parity-conserving sector, F is the "big" enhancement factor that incorporates the PNC matrix element (M_{PNC}), and Q_{exp} is the measured pseudoscalar observable (analyzing power, circular polarization, or gamma asymmetry as explained in the cited references). All the experimental data are taken from Refs. 64 or 132 except those for ^{180}Hf and ^{223}Th, which are taken from Refs. 131 and 125, respectively. The estimations for the PNC matrix elements, if not specified, are performed within the OXBASH code.[63] Exact calculations are not possible in some cases because the isospins and sometimes the spins of some lower-lying states are not known, or the OXBASH code has not quite such good interactions for those cases. In the ^{36}Cl and ^{36}Ar cases, within the D3F7 model space (see Ref. 46), the single-particle contributions to the total PNC matrix elements vanish. Within a larger model space, these contributions are included and such calculations show larger PNC matrix elements (see Sec. 5.4).

Nucleus	$J_1^\pi T_1$	$J_2^\pi T_2$	E_1 (MeV)	E_2 (MeV)	Γ_1 (keV)	Γ_2 (keV)	f	V (eV)	F (10^3)	Q_{exp} (10^{-5})	Refs.
^{10}B	2^-0	2^+1	5.1103	5.1639	1.2	0.002	24.4	0.1	4.6		17
^{13}N	$\frac{3}{2}^-$	$\frac{3}{2}^+$	15.065	14.05	0.86	165	14	0.9	$\simeq 1$		
^{13}N	$\frac{5}{2}^-$	$\frac{5}{2}^+$	11.7	11.53	115	430	1.7	0.9	$\simeq 1$		
^{14}N	0^-1	0^+1	8.796	8.624	410	3.8	10.4	1.04	6.3	0.86	56, 16
^{14}N	2^-0	2^+1	9.3893	9.17225	13	0.135	9.8	0.5	2.5		38
^{14}N	(2^-)	(2^+)	11.67	11.51	150	7	4.6	0.5	1.5		
^{15}O	$\frac{3}{2}^-$	$(\frac{3}{2})^+$	9.609	9.527	8.8	280	5.6	0.2	$\simeq 1.5$		
^{15}N	$\frac{1}{2}^-$	$\frac{1}{2}^+$	11.2928	11.437	8	41.4	2.3	0.8	$\simeq 1.3$		
^{16}O	2^-1	2^+0	12.9686	13.020	1.6	150	9.7	0.1	1.9		34
^{16}O	1^+1	1^-0	16.209	16.20	19	580	5.5	0.1	2.5		42
^{17}O	$\frac{1}{2}^-$	$\frac{1}{2}^+$	6.862	6.356	≤ 1	124	≥ 11	0.6	$\simeq 1$		
^{17}O	$\frac{1}{2}^-$	$\frac{1}{2}^+$	7.99	7.956	270	90	1.73	0.3	$\simeq 1.5$		
^{18}F	0^-0	0^+1	1.08054	1.04155	27.5 ps	2.55 fs	112	0.37	103	80	16
^{18}F	2^-	2^+	6.809	6.811	88	3	5.4	0.5	130		
^{19}F	$\frac{1}{2}^-\ \frac{1}{2}$	$\frac{1}{2}^+\ \frac{1}{2}$	0.109844	0.0	0.85 ns		11	0.46	4.6	-7.1	16
^{19}F	$\frac{3}{2}^-\ \frac{1}{2}$	$\frac{3}{2}^+\ \frac{1}{2}$	1.4587	1.554	90	5	4.3	0.4	1.7		
^{20}Ne	1^-0	1^+1	11.240	11.2623	175		≥ 1	$\simeq 0.5$	≥ 2.5		
^{20}Ne	2^-1	2^+0	11.601	11.885		46	≥ 1	$\simeq 0.8$	≥ 0.8		
^{20}Ne	1^-0	1^+1	13.461	13.484	195	6.4	5.5	0.2	5	150	31
^{21}Ne	$\frac{1}{2}^+\ \frac{1}{2}$	$\frac{1}{2}^-\ \frac{1}{2}$	2.795	2.789	7.6 fs	117 ps	296	0.006	29.6	0.8	16
^{23}Na	$\frac{5}{2}^+\ \frac{1}{2}$	$\frac{5}{2}^-\ \frac{1}{2}$	3.9147	3.818	8 fs	90 fs	6.8	0.3	3.0		30
^{30}P	2^+1	2^-0	4.1826	4.1436	3.2 fs	42 fs	14	1.0	36		30
^{30}P	2^+1	2^-1	7.284	7.224		4.5	≥ 1	$\simeq 0.1$	≥ 0.2		
^{30}Si	2^+1	2^-0	6.537	6.6414	≤ 25 fs	33 fs	≥ 1.15	0.8	$\simeq 1$		
^{36}Cl	2^+1	2^-1	1.95921	1.95105	60 fs	2.6 ps	6.6	≥ 0.1	≥ 8		46
^{36}Ar	2^+	2^-	4.9512	4.974	≤ 50 fs	14 ps	≥ 16	≥ 0.1	≥ 8		46
^{180}Hf	8^-	8^+	1.14161	1.08407	5.5 h	2.18 ps	10^7 (*)	$\simeq 10^{-5}$	10^3	-1660	124
^{223}Th	$\frac{13}{2}^-$	$\frac{13}{2}^+$	0.324	0.320			1.7	$\simeq 0.5$	≥ 21.5		125

(*)The branching ratios (ratios of the partial and total gamma widths) are $b_-=0.1564$ for the M2+E3 transition (the minus sign stands for the negative-parity level of the PMD) and $b_+=0.855$ for the E2 transition (the plus sign stands for the positive-parity level of the PMD), taken from Ref. 131.

eV was achieved with 1.5 days of running time. Several measurements were taken, giving no clear indication of any energy modulation. The measured beam parameters, sensitivities of the apparatus, and false asymmetries are as follows:

Systematic contributions to A_L from coherent beam modulations

Quantity	Measured value	Sensitivity	Resulting false asymmetry
	Spin-independent effects		
Intensity ($\Delta I/2I$)	$\leq 5\cdot10^{-4}$	$-2.1\cdot10^{-3}$	$\leq 1.0\cdot10^{-6}$
Position	$(5\pm2)\cdot10^{-4}$ mm	$-1\cdot10^{-4}$/mm^2	$\leq 1.2\cdot10^{-8}$
Angle	—	$-1.7\cdot10^{-7}$/mrad$^2\cdot\alpha$	—
Width ($\Delta\Gamma/\Gamma$)	$<2\cdot10^{-3}$	$7.5\cdot10^{-4}$	$<1.5\cdot10^{-6}$
Energy	0.3 ± 0.6 eV	$2\cdot10^{-6}$/eV	$(0.6\pm1.2)\cdot10^{-6}$
	Spin-dependent effects		
$(\langle\vec{\varepsilon}\rangle\cdot\langle\vec{p}\rangle)\cdot\hat{z}$	$<2.5\cdot10^{-4}$/mm	$-5.5\cdot10^{-4}$/mm	$<1.4\cdot10^{-7}$
$\langle\vec{\alpha}\rangle\cdot\langle\vec{p}\rangle$	$<6\cdot10^{-4}$/mrad	$2.4\cdot10^{-4}$/mrad	$<1.4\cdot10^{-7}$
$\langle\varepsilon_x p_y\rangle-\langle\varepsilon_y p_x\rangle$	≈ 0.02/mm	$-6.7\cdot10^{-5}$/mm	$\approx 1.3\cdot10^{-6}$
$\langle\alpha_x p_x\rangle-\langle\alpha_y p_y\rangle$	—	$2.0\cdot10^{-5}$/mrad	—

Here $\hat{z}$=nominal chamber axis, $\vec{\varepsilon}$=displacement of beam on target from the z axis, $\vec{\alpha}$=angle of beam on target from the z axis, $\vec{p}$=polarization vector. Sensitivities are for E_p(lab)=1158 keV, 25 μ gm/cm^2 ^{13}C target.

Fortunately, there exists a "magic" energy at which the sensitivity of both the transverse polarization gradients and the energy modulation roughly vanishes. The resulting longitudinal analyzing power is $A_L(b-f)=(0.86\pm0.59)\cdot10^{-5}$ with an estimated systematic error of $0.24\cdot10^{-5}$.

The original calculations ($A_L\approx-2.8\cdot10^{-5}$)[55] on which

the PMD1 experiment in the ^{14}N system was based lead to an isoscalar constraint of opposite sign to the DDH prediction[56] and in better agreement with the ^{21}Ne case than the ^{19}F case when considering the nuclear part of the calculations without problems. It is interesting that in this case the theoretical value of the PNC matrix element decreased with time from 1.37 eV (obtained within a restricted REWIL space[55]), passing through the Haxton value 1.04 eV [Refs. 55 (addendum), 56, and 127] (within the full $\hbar\omega$), and to our value 0.5 eV (within the PSD model space) or smaller.[39] Before extracting a reliable value of the $h_\rho^{(0)}$ coupling constant, we must have confidence in the nuclear-structure and reaction considerations (shell model, scattering theory) used to predict the PNC effect.

The predictions of the analyzing powers depend on the models for the nuclear structure and the nuclear-reaction mechanisms. At present there is no known unique model for both the nuclear-structure and nuclear-reaction parts at the necessary level to describe PNC effects. Therefore, when we calculate the PNC observables by using formulas, such as those given in Refs. 37, 41, 42, 54, and 55, which should not depend on the phases of the wave function used, in reality they will depend on these phases, because we are forced to apply different models for different quantities in these formulas. As an example, within the OXBASH code we calculate the PNC matrix elements and the spectroscopic amplitudes, but not the scattering phases and the partial widths, for which we are forced to apply models given by a specific nuclear-reaction mechanism. For the scattering phases, for instance, we should incorporate in the optical potential terms which are not directly present in the OXBASH code, or at least they may not have the same form (as, e.g., the spin–orbit term, or they may be tensorial terms). The average field and the effective residual interactions present in the OXBASH code are thus prepared in order to work within a bound-state basis. It does not contain continuum or resonance s.p. states or more complicated states, such as the continuum states for two or three reaction fragments. Moreover, the OXBASH code is based on a s.p. oscillator potential, which always produces bound states. Some other codes[119] are sometimes based on a more realistic Saxon–Woods bound-state basis; however, the continuum states are also not incorporated in such codes. The only approach which takes care of both bound and continuum s.p. states is the shell-model approach to nuclear reactions;[120] however, within this approach the residual interactions cannot be included easily, and the PNC observables cannot be estimated without incorporating the residual interactions in the model calculations.

Using our PNC matrix element (0.5 eV), the agreement between the experimental and theoretical magnitudes of the largest energy anomaly ($\Delta A_{L(b)}$) is better; however, neither in Ref. 55 nor in our work was the contribution from the recently proposed[96] s.p. PNC matrix element calculated.

From these calculations we may learn the following facts: (i) The PNC matrix element is dominated by the $h_\rho^{(0)}$ term. This becomes three times smaller in the Kaiser and Meisner chiral-soliton theory than the DDH "*best values*" (see Table II for a comparison with other theories for weak vertices). (ii) The refinements in the structure part of the PNC matrix element have been carefully discussed in Refs. 39 and 56. The new s.p. term proposed by Caprini and Micu may also reduce the total PNC matrix element. All these ingredients may reduce the total matrix element by 40%, and the $h_\rho^{(0)}$ obtained in Ref. 16 could, in principle, describe the experimental data.[56] (iii) A new measurement of the longitudinal analyzing power for this case is necessary in order to strengthen the conclusions based on the experimental value of Ref. 56. A new measurement is proposed[121] at an angle $\theta_{CM}=100°$, where the quantity $\sigma(\theta_{CM})\cdot A_L^2(\theta_{CM})$ (proportional to the measuring time for a defined precision) has a maximum in the backward region.

TABLE II. Weak meson–nucleon coupling constants calculated within different weak-interaction models (in units of 10^{-7}). The abbreviations are: KM=Kaiser and Meissner,[15] DDH=Desplanques, Donoghue, and Holstein "best" values,[13]. AH=Adelberg and Haxton,[16] and DZ=Dubovik and Zenkin.[14]

$h_{\text{meson}}^{(\Delta T)}$	KM	DDH	AH (fit)	DZ
$h_\pi^{(1)}$	0.19	4.54	2.09	1.30
$h_\rho^{(0)}$	−3.70	−11.40	−5.77	−8.30
$h_\rho^{(1)}$	−0.10	−0.19	−0.22	0.39
$h_\rho^{(2)}$	−3.30	−9.50	−7.06	−6.70
$h_{\rho'}^{(1)}$	−2.20	0.00	0.00	0.00
$h_\omega^{(0)}$	−1.40	−1.90	−4.97	−3.90
$h_\omega^{(1)}$	−1.00	−1.10	−2.39	−2.20

The PMD2 case has other problems. Because of the small width (0.135 keV) of the 2^+1 9.17225-MeV level, the energy anomaly of the PNC analyzing powers is a nonzero quantity in only a very small[41] energy range ($\leqslant$1 keV), and it is of the order of some units above 10^{-5} within the DDH +PSDMK (Millener–Kurath interaction).[13,63] By considering the $2^\pm$ PMD in ^{14}N, analyzed via the circular polarization of 9.3893-MeV γ rays, we came to realize that this observable is equal to $1.04\cdot10^{-3}$ in the case of an unoriented 2^- $T=0$ state and with zero mixing ratios. This value has been obtained by calculating, within the OXBASH code (Millener–Kurath interaction), the 9.3893-MeV E1+M2 γ-emission probability ($2.886\cdot10^{12}$ s^{-1}) and the 9.17225-MeV M1+E2 γ-emission probability ($3.036\cdot10^{16}$ s^{-1}). The last value (Γ_γ=24.4 eV) is in agreement with the measured value (Γ_γ=7 eV).[122] Unfortunately, there is no measured value for the E1+M2 γ emission. This high value of the circular polarization can be explained by a high hindered E1 transition, which is isospin-forbidden. This measurement has, however, a very small probability, because of an almost 100% proton decay probability of the 2^-0 9.3893-MeV state; however, it could be performed as in the ^{19}F experiment.

4.2. Parity mixing in ^{16}O

The ^{16}O energy spectrum contains two (see Table I) isovector PMDs,[64] one ($\Delta E\approx$50 keV) at 13 MeV excitation energy,[34,35] and one ($\Delta E\approx$9 keV) at 16.2 MeV excitation energy.[42]

These PMDs can be explored by measuring two components of the vector analyzing power: A_L and A_b, for which a careful theoretical analysis was made, and the results are

$A_L^{\mathrm{PMD1}}=1.4\cdot 10^{-5}$, $A_b^{\mathrm{PMD1}}=0.9\cdot 10^{-5}$ (Ref. 34), $A_L^{\mathrm{PMD2}}=(3.2\times 10^{-5})$, and $A_b^{\mathrm{PMD2}}=2.3\cdot 10^{-5}$ (Ref. 42) for large angles ($\simeq 150°$).

We want to discuss the first PMD in more detail, since it has been the subject of our group's special attention[34] as the best candidate for a new isovector experiment. The α_0 transition from the $J^\pi T=2^-1$ state in ^{16}O ($E_x=12.9686$ MeV, $\Gamma_{\mathrm{cm}}=1.6\pm 0.1$ keV), populated by resonant capture of polarized protons ($E_p=0.898$ MeV), to ^{12}C (g.s.) was thoroughly investigated theoretically.[34] This transition has originally been mentioned by Bizzeti and Maurenzig.[123] The α_0 transition is forbidden by parity and, partially, by isospin selection rules. It can therefore be predominantly described by the isovector part of the PNC-NN potential (mainly one-pion exchange), thus being sensitive to the weak πNN coupling constant $h_\pi^{(1)}$.

The excitation functions of the PNC longitudinal (A_L) and PNC transverse (A_b) analyzing powers are expected (Refs. 31, 32, 37, 54, 55, and 123) to show an energy anomaly at the 2^-1 resonance energy due to the interference of the forbidden (PNC: 2^-1, 12.9686 MeV) and allowed (PC: 2^+0, 13.020 MeV; 1^-1, 13.090 MeV) resonance transition amplitudes as well as a (PC: 0^+0) background transition amplitude. The level structure of the ^{16}O nucleus[64] enhances the interference effect because of the close-lying ($\Delta E=51$ keV) broad overlapping 2^+0 state at $E_x=13.020$ MeV with $\Gamma_{\mathrm{cm}}=150\pm 10$ keV.

Following Ref. 44, where a more rigorous approach to the parity-forbidden alpha decay is proposed, it is possible to estimate the order of magnitude of the weight of the admixtures from different 2^+0 levels in the 2^-1 level as the product

$$F_n S_{\alpha n}^{1/2}=|(E^{2^-1}-E^{2^+0})^{-1}\langle 2^-1|H_{\mathrm{PNC}}|2_n^+0\rangle S_{\alpha n}^{1/2}|, \quad (30)$$

where $S_{\alpha n}^{1/2}$ is an SU(3) alpha-particle amplitude.[63] The results are listed in Ref. 34. From these values we conclude that the assumption of a parity-mixed doublet (2^-1, 12.9686 MeV and 2^+0, 13.020 MeV excited states in ^{16}O) is justified. In this case, the expression for the PNC T matrices obtained by expanding the exact Green's function[37,54,55] to first order in H_{PNC} is certainly a good approximation. It is assumed that the projectile and the target are parity eigenstates. Then PNC contributions from direct reaction terms are ignored, and only effects related to the closeness of the two resonances are taken into account. The resonance parameters for the quantities in the equations for $A_{L(b)}$ are given in Ref. 34.

The parity mixing of the above-mentioned doublet is of particular interest because:

(1) The mixing is sensitive to the $\Delta T=1$ components of H_{PNC} and especially to the long-range part described by weak pion exchange, taking the quark-model picture. In this case quantitative information about neutral-current contributions to H_{PNC} is expected. Several cases have been proposed theoretically, but only a few of them have been experimentally investigated; only the ^{18}F experiments (average of five investigations)[16] give a reliable upper limit for the weak pion–nucleon coupling constant. Taking into account the recent sophisticated shell-model calculation,[29,43] the result is not in contradiction with the predictions of Refs. 13–15; however, additional investigations are necessary, especially with independent observables.

(2) The polarization observables for the $^{15}\mathrm{N}(\vec{p},\alpha_0)^{12}\mathrm{C}$ reaction provide a favorable way to determine the PNC matrix elements. The energy anomaly in the PNC analyzing powers (A_L and A_b) is magnified by nuclear-structure effects in addition to the 51-keV energy difference between the levels involved. The magnification arises from coherent contributions of the proton and α channels. The quantity $C_{L(b)}$ describes the ratio of the PC T-matrix contribution to the PNC analyzing powers and the (unpolarized) cross section for the $(\vec{p},\alpha)$ reaction (see Ref. 34). The value of this ratio is about 0.1 in the resonance region, being a measure of the coherence effect. The width of the 2^-1 resonance level is very small (1.6 keV) and also acts as an enhancement factor. The ratio $\Gamma_p^{2^-}/\Gamma_p^{2^+}$ has the value 3.4 and is another enhancement factor, as was pointed out in Ref. 55 (similar ratios of unnatural- to natural-parity level widths are of the order of 10^{-2} (see, e.g., Ref. 64).

(3) The cross section for the $^{15}\mathrm{N}(\vec{p},\alpha_0)^{12}\mathrm{C}$ case is maximal at backward angles.[126] Moreover, the normal PC analyzing power is negligibly small[126] in this energy region for large scattering angles, which is a favorable situation for measurement. Furthermore, the α channel can be studied more precisely than, e.g., the case of PNC elastic scattering (target impurities, systematic asymmetries due to energy modulations and transverse polarization gradients,[56] reduced number of α channels, etc.).

(4) The PNC α_0 transition can be studied via the $^{15}\mathrm{N}(\vec{p},\alpha_0)^{12}\mathrm{C}$ resonance reaction with two polarization observables, namely, the PNC longitudinal and PNC transverse analyzing powers A_L and A_b. Information about the PNC matrix element can be obtained independently from the excitation energy of each observable. Up to now, only the case of the $^{19}\mathrm{F}(\vec{p},\alpha_0)^{16}\mathrm{O}$ reaction has been studied experimentally,[31–33] giving an upper limit[31] on the corresponding PNC asymmetry.

(5) The theoretical models included in the OXBASH code are reasonably good (see Refs. 34 and 35) for the levels of the above-mentioned $2^-,2^+$ doublet, since the even–even ^{16}O nucleus is an often used candidate, being well described by such realistic models. In particular, the (first) excited $J^\pi=2^-1$ state can be reliably reproduced.

These conclusions are based on the following investigations. Because of the small proton energy, the angular momentum can be restricted to $l\leqslant 2$. Together with the spins and parities of the participating nuclei, the following four PC transition amplitudes are allowed:

$$t_1=T_{bg}=T_{\alpha 00,p11}^{0^+}; \quad t_2=T_{\alpha 10,p01}^{1^-};$$
$$t_3=T_{\alpha 10,p21}^{1^-}; \quad t_4=T_{\alpha 20,p11}^{2^+}. \quad (31)$$

Two PNC transition amplitudes are taken into account:

$$T_1=T_{\alpha,20,p20}^{2^+,-}; \quad T_2=T_{\alpha 20,p21}^{2^+,-}. \quad (32)$$

The general form of the PC resonance T-matrix elements is

$$T^{J^\pi}_{\beta ls,\beta_1 l_1 s_1}=\frac{i\exp(i\xi_{\beta ls})\sqrt{\Gamma^{J^\pi}_{\beta ls}}\sqrt{\Gamma^{J^\pi}_{\beta_1 l_1 s_1}}\exp(i\xi_{\beta_1 l_1 s_1})}{E-E^{J^\pi}+\frac{i}{2}\Gamma^{J^\pi}}, \tag{33}$$

$$T^{J^\pi,-\pi}_{\beta ls,\beta_1 l_1 s_1}=\frac{i\exp(i\xi_{\beta ls,\beta_1 l_1 s_1})\sqrt{\Gamma^{J^{-\pi}}_{\beta ls}}\langle J^{-\pi}|H_{\rm PNC}|J^\pi\rangle\sqrt{\Gamma^{J^\pi}_{\beta_1 l_1 s_1}}\exp(i\xi_{\beta_1 l_1 s_1})}{\left(E-E^{J^{-\pi}}+\frac{i}{2}\Gamma^{J^{-\pi}}\right)\left(E-E^{J^\pi}+\frac{i}{2}\Gamma^{J^\pi}\right)}. \tag{34}$$

Here β (β_1) stands for α (p); $\xi_{\alpha(p)ls}$, E^{J^π}, and Γ^{J^π} are the α (p) channel phases, resonance energies, and total resonance widths, respectively; E is the proton energy in the compound system. The quantities $\sqrt{\Gamma^{J^\pi}_{\alpha(p)ls}}$ are taken from experiments[64,126] if available; otherwise they are expressed in terms of the OXBASH spectroscopic amplitudes,[63] geometrical coefficients, and s.p channel widths.

The calculations within the OXBASH code gave the following results:

$$\left|\frac{\sqrt{\Gamma^{1^-}_{p21}}}{\sqrt{\Gamma^{1^-}_{p01}}}\right|=2\cdot 10^{-3};\quad \Gamma^{1^-}_{p01}\simeq\Gamma^{1^-}_{p}(\text{exp})=100\ \text{keV}; \tag{35}$$

$$\left|\frac{\sqrt{\Gamma^{2^-}_{p20}}}{\sqrt{\Gamma^{2^-}_{p21}}}\right|=1;\quad \Gamma^{2^-}_{p20}=\Gamma^{2^-}_{p21}=\frac{1}{2}\Gamma^{2^-}_{p}(\text{exp})=0.495\ \text{keV}; \tag{36}$$

$$\Gamma^{2^+}_{p11}=\Gamma^{2^+}_{p}(\text{exp})=3.4\ \text{keV}. \tag{37}$$

It turns out that $T_1=T_2$. Contributions from the spin–orbit potential to the proton channel phases and spectroscopic amplitudes have been neglected in view of the low proton energy ($E_p\simeq 900$ keV).

In the following we discuss the degree of accuracy of the shell-model calculations within the available OXBASH code in order to substantiate the opinion that the experimental results on the PNC analyzing powers of the $^{15}\text{N}(\vec{p},\alpha_0)^{12}\text{C}$ resonance reaction with $E_p\simeq 0.898$ MeV can be analyzed without nuclear-structure uncertainties.

In order to predict the magnitude of the effect and to check the feasibility of an experiment to measure A_L and/or A_b around the resonance energy of the first excited 2^-1 state in ^{16}O, we calculated the matrix element

$$\langle 2^-1,\ 12.9686\ \text{MeV}|H_{\rm PNC}|2^+0,\ 13.020\ \text{MeV}\rangle \tag{38}$$

using the OXBASH code in the Michigan State University version,[63] which includes different model spaces and different residual effective two-nucleon interactions.

Two different model spaces have been used: the ZBM and PSD model spaces (see Sec. 3). In order to maintain the matrix dimensions at a nonprohibitive level, the nucleons were considered to be frozen in the $1p_{3/2}$ orbit; thus, a fixed $(1s_{1/2})^4(1p_{3/2})^8$ configuration is assumed in all cases. It turns out that at least four-particle–four-hole calculations are needed[16,127,128] in order to describe the 2^+ states in ^{16}O.

Five different residual interactions have been used in the ZBM model space: ZBM I, ZBM II, REWIL, ZWMO, and ZWM. Two different combinations of interactions have been taken into account in the PSD model space: PSDMK, PSDMWK. While the center-of-mass spuriosity is small in the ZBM model space, the number of spurious components is high in the PSD space, but the degree of spuriosity of every component is small. In PSDMK+CM and PSDMWK+CM the contributions of spurious components were eliminated by a procedure analyzed in Ref. 118.

The one-body part [see Eq. (15)] of the PNC matrix element turns out to be dominant in all the cases described above.

The TBME have been calculated with harmonic-oscillator wave functions ($\hbar\omega=14$ MeV is appropriate for $A=16$).[25]

The short-range correlations (SRC) of the shell-model wave function were implemented by multiplying the radial two-body wave function by a kind of Jastrow factor (see Sec. 3). Table II of Ref. 35 gives the nuclear-structure parts of the PNC matrix element, with and without SRC, and, separately, the single- and two-particle contributions.

Moreover, recent experimental measurements[129,130] showed a relatively strong isospin mixing of the 2^-1, $E_x=12.9686$ MeV level with the 2^-0, $E_x=12.53$ MeV level in ^{16}O*. In Ref. 35 it was shown that the isospin impurity of the 2^-, $T=0$, $E_x=12.53$ MeV level in the 2^-, $T=1$, $E_x=12.9686$ MeV level does not change significantly the results of Ref. 34, i.e., the PNC analyzing powers increase by $\approx 30\%$ if one takes the sign of the isospin impurity as given in Eq. (1) of Ref. 35.

In these calculations the standard form for $H_{\rm PNC}$ has been used (see Sec. 2), with the weak coupling constants given in Tables II and III. The strong coupling constants are summarized in the last four columns of Table II from Ref. 15. The calculated PNC matrix elements for different weak-interaction models and different shell-model residual interactions are shown in Table IV. As can be seen, the results for different interactions agree within a factor of 2.5, and no large suppression appears when the model space is enlarged. The ρ and ω exchange contributions add coherently to the total matrix element in every case.[34,35] The contributions

TABLE III. The expressions for the coefficients $F_{k,s}^{(\Delta T)}$ multiplying the matrix elements $M_{k,s}^{(\Delta T)}$ [see Eq. (14)] are noted in the first column. Numerical values (in units of 10^{-6}) are given for the "best" values of the PNC meson–nucleon couplings in the DDH approach,[13] as well as the values obtained by Kaiser and Meissner.[15]

$F_{k,s}^{(\Delta T)}$	KM	DDH
$F_{0,\pi}^{(1)}=\frac{1}{2\sqrt{2}}\, g_\pi h_\pi^{(1)}$	0.090	2.16
$F_{1,\rho}^{(1)}=-\frac{1}{2}\, g_\rho h_\rho^{(1)}$	0.014	0.027
$F_{2,\rho}^{(1)}=-\frac{1}{2}\, g_\rho h_\rho^{1}(1+\mu_v)$	0.066	0.127
$F_{3,\rho}^{(1)}=\frac{1}{2}\, g_\rho h_\rho^{(1)}$	−0.014	−0.027
$F_{1,\omega}^{(1)}=-\frac{1}{2}\, g_\omega h_\omega^{(1)}$	0.437	0.480
$F_{2,\omega}^{(1)}=-\frac{1}{2}\, g_\omega h_\omega^{(1)}(1+\mu_s)$	0.384	0.423
$F_{3,\omega}^{(1)}=-\frac{1}{2}\, g_\omega h_\omega^{(1)}$	0.437	0.480
$F_{4,\rho}^{(0)}=-g_\rho h_\rho^{(0)}(1+\mu_v)$	4.850	14.94
$F_{5,\rho}^{(0)}=-g_\rho h_\rho^{(0)}$	1.032	3.180
$F_{6,\omega}^{(0)}=-g_\omega h_\omega^{(0)}(1+\mu_s)$	1.038	1.408
$F_{7,\omega}^{(0)}=-g_\omega h_\omega^{(0)}$	1.179	1.6
$F_{0,\rho}^{(1)}=-\frac{1}{2}\, g_\rho h_{\rho'}^{(1)}$	0.307	0.0
$F_{8,\rho}^{(2)}=-\frac{1}{2\sqrt{6}}\, g_\rho h_\rho^{(2)}$	0.886	2.542
$F_{9,\rho}^{(2)}=-\frac{1}{2\sqrt{6}}\, g_\rho h_\rho^{(2)}$	0.189	0.541

from heavy mesons do not exceed 25% for the DDH, AH, and DZ cases but increase to 50% in the KM model, reducing the contribution of pion exchange. If this model is taken at face value, the chance of observing a trace of $h_\pi^{(1)}$ is considerably decreased.

Considering the present discrepancies between the DDH values[13] and the KM results,[15] the conservative choice of the matrix element $\langle 2^-1|H_{\rm PNC}|2^+0\rangle \simeq 0.1$ eV is consistent with the DZ model[14] and is also supported by $\Delta T=1$ PNC experiments.[16] In this case 75% of the value arises from pion exchange. The contribution of the new class of diagrams in the PNC single-particle Hamiltonian recently proposed by Caprini and Micu[96] vanishes for the proposed matrix element.

It is essential to compare the predictions of the above theoretical model with the experimental results for the cross section and the (regular) analyzing power of the ^{15}N$(p,\alpha)^{12}$C reaction. The resonance parameters used for the PC T matrices are taken from the latest compilation.[64] The proton phases ξ_{pls} have been calculated by a folding procedure, using a realistic M3Y interaction.[44] The results are very close to the Coulomb phases. The α channel phases and the background PC 0^+0 T-matrix element $t_1=t\exp(i(\alpha))$ have been fitted to reproduce the Legendre-polynomial coefficients for the cross section and the PC analyzing power of Pepper and Brown.[126] The expansion coefficients extracted from experiment and from the present investigation (see Ref. 34) show the quality of the theoretical treatment. The calculation of the PNC analyzing powers A_L and A_b has been performed with the same parameters. The PNC analyzing power shows a dispersion-like energy behavior around the resonance energy, whose form depends on the phase difference of the contributing matrix elements. However, the difference between the maximum and the minimum is equal to the quantity $D_{L(b)}$ defined in Eq. (26). It is a very important fact that this quantity depends neither on the phase $\phi_{\rm PNC}$ nor on the PC phase $\phi_{L(b)}$ of $C_{L(b)}$.

In Fig. 1 (a,b,c,d) we show on an expanded horizontal scale the predicted size of the quantities relevant for an experiment designed to determine the PNC matrix element by measurement of A_L and/or A_b around the narrow 2^-1 resonance. The information on the modulus of the PNC matrix element can therefore be extracted from $A_{L(b)}$ measurements.

On the basis of these predictions an experimental proposal to measure the PNC analyzing powers A_L (and A_b) in the ^{15}N$(\vec{p},\alpha_0)^{12}$C reaction is sketched in the following. At backward scattering angles the (PC) analyzing power A_n is very small or even zero,[126] whereas the cross section is maximal in the relevant energy region around $E_{\rm res}(2^-1)\approx E_p=898$ keV. This situation is favorable for PNC asymmetry measurements because several PC asymmetry effects, superimposed on the PNC observables, are small if A_n is small. Moreover, this advantage coincides with the maximum of the predicted PNC interference effect in A_L [e.g., $\Delta A_L(\theta_{\rm CM}=160°)=2.6\cdot 10^{-5}$]. Although A_b is smaller than A_L in many experimental cases, it has a comparable size near $\theta=90°$. However, at this angle the differential cross section appears to be smaller than its magnitude at large angles.[34] Therefore, and because of the solid-angle restriction in the A_b measurement (detectors only in one reaction plane), the observable A_L is the more favorable one for the realization of a PNC experiment.

TABLE IV. The PNC matrix element for PMD1 in ^{16}O, calculated for different weak and strong interactions. The abbreviations are discussed in the text.

	DDH			AH			DZ		
Interactions	V_π	$V_{\rho(\omega)}$	$V_{\rm tot}^{\rm DDH}$	V_π	$V_{\rho(\omega)}$	$V_{\rm tot}^{\rm AH}$	V_π	$V_{\rho(\omega)}$	$V_{\rm tot}^{\rm DZ}$
ZBM I	−0.287	−0.016	−0.303	−0.138	−0.028	−0.166	−0.086	−0.021	−0.107
ZBM II	0.660	0.036	0.696	0.306	0.061	0.367	0.189	0.047	0.236
REWIL	0.332	0.017	0.349	0.154	0.290	0.183	0.095	0.023	0.118
ZWM	−0.709	−0.037	−0.746	−0.328	−0.064	−0.392	−0.204	−0.050	−0.254
PSDMK	−0.381	−0.014	−0.395	−0.176	−0.029	−0.205	−0.109	−0.022	−0.131
PSDMK+CM	0.304	0.021	0.325	0.141	0.041	0.182	0.087	0.031	0.118
PSDMWK	0.437	0.020	0.457	0.202	0.040	0.242	0.125	0.031	0.156
PSDMWK+CM	0.423	0.025	0.448	0.196	0.049	0.245	0.122	0.037	0.159

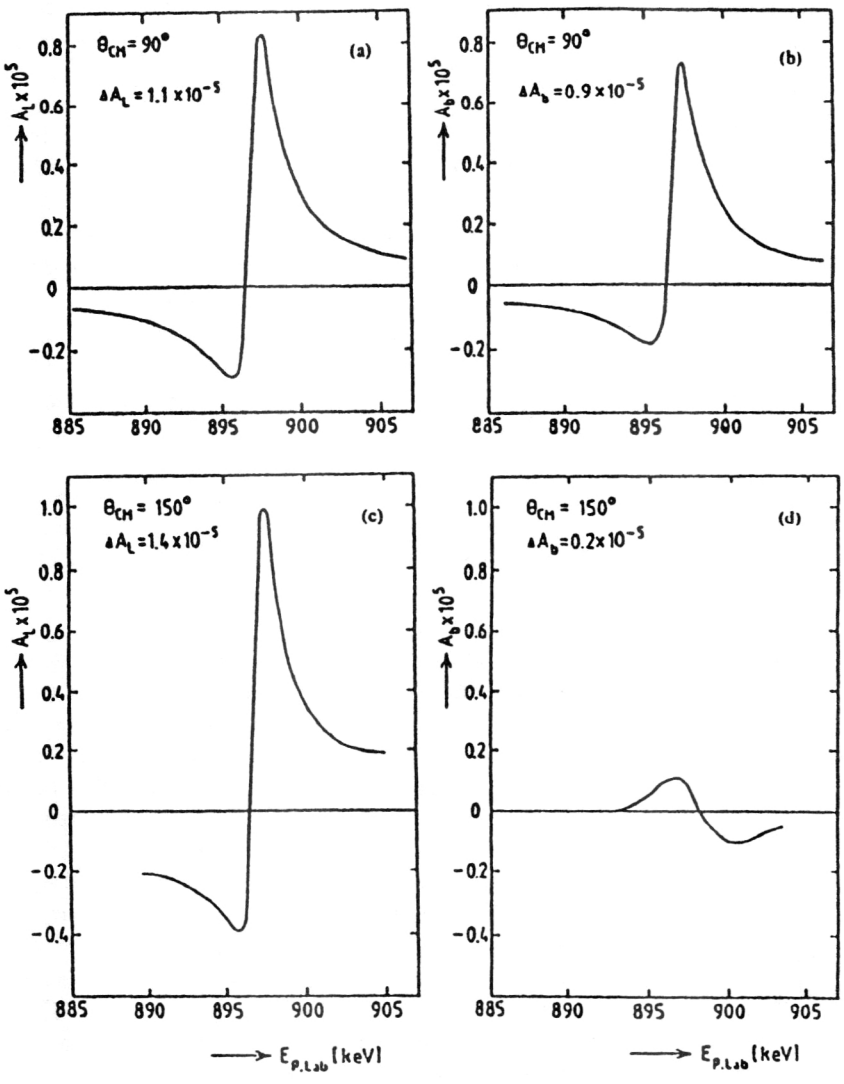

FIG. 1. (a,b,c,d): Longitudinal and irregular transverse analyzing powers of the reaction $^{15}N(\vec{p},\alpha_0)^{12}C$ versus the proton energy, for θ=90° and 150° around the proton energy $E_p^{LAB}\approx 0.9$ MeV (M_{PNC}=0.1 eV).

The small width of the 2^- level at E_p=898 keV requires a thin ^{15}N target ($\Delta E \leq 1$ keV for E_p=898 keV), e.g., realized by implanting ^{15}N ions on the surface of a Ti backing or preparing a thin Ti^{15}N target layer, as was done in Ref. 36. Another possibility is the use of a ^{15}N gas target. It has the advantage that the energy loss in the target gas can be adjusted in such a way that one can measure five different energy points around the resonance energy simultaneously. In this case up to 20 Si surface-barrier detectors (or parallel-plate avalanche counters) can be installed in five rings around a long target gas tube, e.g., at $\theta_{Lab}=(135\pm24)°$ or $\theta_{Lab}=(90\pm24)°$, as well as at lower energies with large solid angles ($0.4\leq\Omega\leq0.6$ sr). The azimuthal angles ϕ=0°, 90°, 180°, and 270° have been chosen to be sensitive for (on-line) monitoring of spurious asymmetries caused by residual transverse polarization components of the beam. The scattered particles leave the gas tube through aluminum foils (12–15 μm), which are used in front of the detectors in order to stop elastically scattered protons and low-energy α_1 particles from excited ^{12}C states, providing background-free α_0 spectra. The reaction energy can be adjusted precisely by detecting the γ rays from the $^{15}N(\vec{p},\gamma)^{16}O^*$ reaction. These spectra serve at the same time as a monitor for detecting carbon built-up products on the entrance foil of the gas tube, to correct for this time-dependent additional energy loss of the proton beam. The entrance foil is a self-supporting carbon layer of $\leq$60 nm thickness in order to minimize the energy loss and straggling of the proton beam. This is essential because of the small resonance width of the 2^- level. Selecting an energy resolution of the polarized proton beam of $\approx\pm0.6$ keV, provided by two narrow feedback slit systems, and adjusting the target gas pressure to $\approx$1.3 mbar, the measurement can be performed at five energies simultaneously within the interval $E_{res}-\frac{3}{2}\Gamma\leq E_{res}\leq E_{res}+\frac{3}{2}\Gamma$. With an experimental setup of this type a statistical accuracy of $\approx0.3\cdot10^{-5}$ and $\approx0.5\cdot10^{-5}$ will be reached for $A_L(135\pm24)°$ and $A_L(90\pm24)°$, respectively, after 48 μA·d of integrated beam charge, if the helicity of the proton beam is switched between $\pm P_z$ with $P_z\geq0.70$. In order to achieve a sufficient experimental accuracy, the experiment requires a proton beam with high intensity, polarization, and energy resolution. Owing to the low target gas pressure and the high energy resolution restricted by the small resonance width, it is advantageous to improve the experimental setup by use of a differentially pumped gas target without an entrance foil.

Investigations concerning the second isovector PMD in

TABLE V. The PNC matrix element for PMD2 in ^{16}O, calculated for different weak and strong interactions. The abbreviations are discussed in the text.

	KM			DDH			AH			DZ		
Interactions	V_π	$V_{\rho(\omega)}$	$V_{\text{tot}}^{\text{KM}}$	V_π	$V_{\rho(\omega)}$	$V_{\text{tot}}^{\text{DDH}}$	V_π	$V_{\rho(\omega)}$	$V_{\text{tot}}^{\text{AH}}$	V_π	$V_{\rho(\omega)}$	$V_{\text{tot}}^{\text{DZ}}$
ZBMI	−0.006	−0.012	−0.019	−0.168	−0.012	−0.181	−0.070	−0.024	−0.094	−0.044	−0.018	−0.062
ZBMO	−0.031	−0.033	−0.064	−0.748	−0.030	−0.778	−0.344	−0.059	−0.404	−0.214	−0.047	−0.261
ZWM	−0.024	−0.019	−0.043	−0.574	−0.030	−0.604	−0.264	−0.034	−0.298	−0.164	−0.027	−0.019
REWIL	−0.011	−0.006	−0.018	−0.285	−0.005	−0.291	−0.131	−0.011	−0.142	−0.081	−0.009	−0.090
ZBMII	−0.002	+0.001	−0.002	−0.064	+0.001	−0.064	−0.030	+0.001	−0.028	−0.018	+0.001	−0.018

^{16}O have been performed in Ref. 42. Within the shell-model code (OXBASH) with the ZBM model space and different interactions (see Table V), we calculated the PNC matrix element and PNC analyzing powers (A_L and A_b). The average value for the PNC matrix element is 0.4 eV. The maximum in the energy anomaly of the PNC analyzing powers (A_L and A_b) was found to be some units above the 10^{-5} value considered to be in agreement with the last measurements,[19,56] [see Fig. 2 (a,b,c,d)].

5. GAMMA ASYMMETRIES

The degree of circular polarization (helicity asymmetry) of the emitted γ rays is given (see Ref. 133, Chap. 9, §3, Eq. (9.38)] by a sum of parity-nonconserving (PNC) and parity-conserving (PC) contributions,

$$P_\gamma(\cos\theta)\equiv\frac{W_{\text{right}}(\theta)-W_{\text{left}}(\theta)}{W_{\text{right}}(\theta)+W_{\text{left}}(\theta)}=\Bigg(\sum_{LL'\nu}B_\nu(I)F_\nu(LL'I'I)$$
$$\times[\delta_{L+L'+\nu,\text{odd}}(m_L^*m_{L'}+e_L^*e_{L'})$$
$$+\delta_{L+L'+\nu,\text{even}}(m_L^*e_{L'}+e_L^*m_{L'}]P_\nu(\cos\theta))$$
$$\times\Bigg(\sum_{LL'\nu}B_\nu(I)F_\nu(LL'I'I)$$
$$\times[\delta_{L+L'+\nu,\text{even}}(m_L^*m_{L'}+e_L^*e_{L'})$$
$$+\delta_{L+L'+\nu,\text{odd}}(m_L^*e_{L'}+e_L^*m_{L'})]P_\nu(\cos\theta)\Bigg)^{-1}$$
$$=(P_\gamma)_0\cdot R_\gamma^{\text{PNC}}(\cos\theta)+R_\gamma^{\text{PC}}(\cos\theta), \tag{39}$$

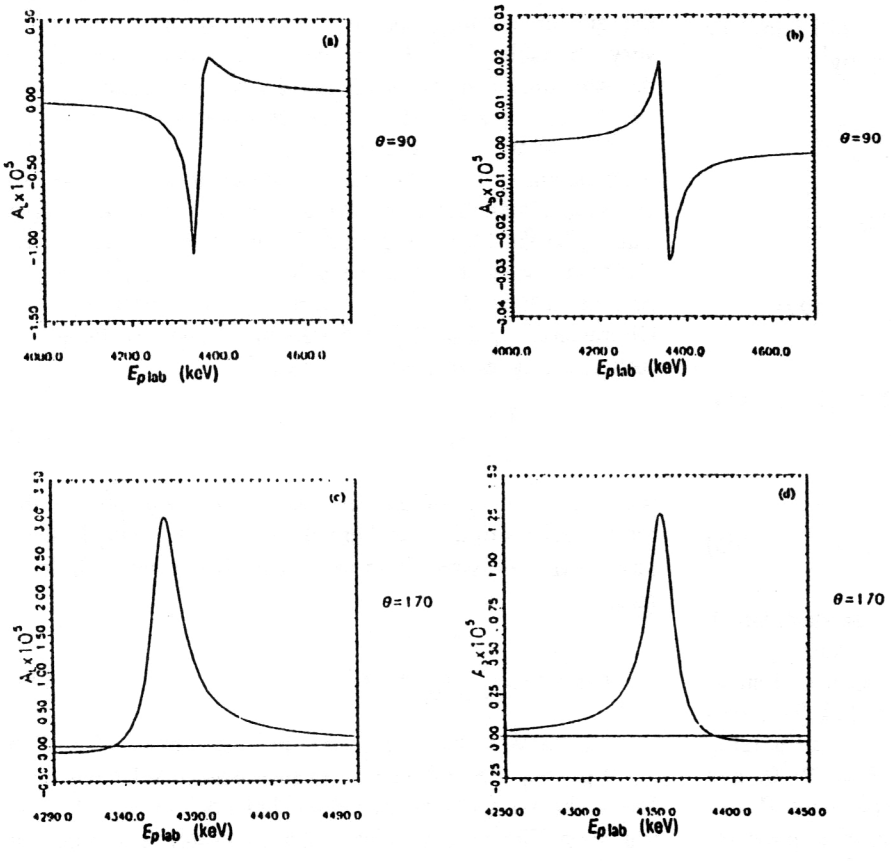

FIG. 2. (a,b,c,d): Longitudinal analyzing power of the reaction $^{15}\text{N}(\vec{p},\alpha_0)^{12}\text{C}$ versus the proton energy for θ=90° and 170° around the proton energy $E_p^{\text{LAB}}\approx$4.35 MeV (M_{PNC}=0.4 eV).

and the circular polarizations for an unpolarized initial nucleus with zero and finite mixing ratios,[134] respectively, are

$$(P_\gamma)_0 = 2\cdot \frac{M_{\rm PNC}}{\Delta E}\sqrt{\frac{b_+\cdot\tau_-}{b_-\cdot\tau_+}}\cdot\left(\frac{E_\gamma^-}{E_\gamma^+}\right)^3, \tag{40}$$

$$(P_\gamma)_{un} = (P_\gamma)_0\cdot\sqrt{\frac{1+\delta_-^2}{1+\delta_+^2}}. \tag{41}$$

Here $R_\gamma^{\rm PNC}$ is a factor due to the existence of the orientation of the nucleus in the initial excited state when the mixing ratios do not vanish, which, for instance, in the case of $A=36$ gamma transitions is given by[30,46,47]

$$\begin{aligned} R_\gamma^{\rm PNC}(\cos\theta) = \sqrt{\frac{1+\delta_-^2}{1+\delta_+^2}}\Bigg\{\sum_{\nu=0,2,4} P_\nu(\cos\theta)B_\nu(2) \\ \times[F_\nu(1122)+F_\nu(2222)\delta_+\delta_+ + F_\nu(1222) \\ \times(\delta_- + \delta_+)]\Bigg\}\cdot\Bigg\{\sum_{\nu=0,2,4} P_\nu(\cos\theta)B_\nu(2) \\ \times[F_\nu(1122)+F_\nu(2222)\delta_-^2 \\ +2F_\nu(1222)\delta_-]\Bigg\}^{-1}, \end{aligned} \tag{42}$$

where the coefficients F_ν are defined by

$$\begin{aligned} F_\nu(LL'I'I) = (-1)^{I'+3I-1}[(2I+1)(2L+1)(2L'+1)]^{1/2} \\ \times C(LL'\nu;1-10)W(LL'II;\nu I'), \end{aligned} \tag{43}$$

in which C is the Clebsch–Gordan coefficient $C(J_1J_2J_3;M_1M_2M_3)$ and W is the Racah coefficient. The parity-conserving (PC) γ asymmetry is given by[133]

$$\begin{aligned} R_\gamma^{\rm PC}(\cos\theta) = \Bigg\{\sum_{\nu=1,3} P_\nu(\cos\theta)B_\nu(2)[F_\nu(1122) \\ +F_\nu(2222)\delta_-^2 + 2\cdot F_\nu(1222)\delta_-]\Bigg\} \\ \times\Bigg\{\sum_{\nu=0,2,4} P_\nu(\cos\theta)B_\nu(2)[F_\nu(1122) \\ +F_\nu(2222)\delta_-^2 + 2F_\nu(1222)\delta_-]\Bigg\}^{-1}, \end{aligned} \tag{44}$$

where

$$B_\nu(2) = \sum_M (2\nu+1)^{1/2}C(2\nu 2;M0M)p(M). \tag{45}$$

Here $p(M)$ is the polarization fraction of the M state, which determines the degree of orientation of the nucleus.

In order to measure a PNC effect, one must find situations for which the $R_\gamma^{\rm PC}$ part in Eq. (40) vanishes. Two particular cases have this property: (i) The case of an initially unpolarized nucleus for which $B_0(2)=1$, $B_{\nu\neq 0}(2)=0$, and $F_0(LL'22)=\delta_{LL'}$. In this particularly simple case P_γ reduces to the well known expression for the circular polarization, $(P_\gamma)_{un}$. (ii) One may prepare a polarized state by choosing $p(M)=\delta_{M0}$, for which $B_{\nu=1,3}(2)=0$ and the $R_\gamma^{\rm PC}$ part vanishes.

Another observable which measure a PNC effect is the forward–backward asymmetry of the gamma rays emitted by polarized nuclei:

$$A_\gamma(\theta) \equiv \frac{W(\theta)-W(\pi-\theta)}{W(\theta)+W(\pi-\theta)}. \tag{46}$$

This observable has been successfully used in the ^{19}F case[18,19] in order to avoid the small efficiency of the Compton polarimeters when one measures the degree of circular polarization. If the mixing ratios are small ($\delta_+, \delta_- \ll 1$), one can show that[39]

$$A_\gamma(\theta) \simeq (P_\gamma)_0\cdot R_\gamma^{\rm PC}(\cos\theta). \tag{47}$$

The angular distribution described by this formula has a maximum at $\theta=0°$.[39] It has the advantage that the parity-conserving (PC) circular polarization $R_\gamma^{\rm PC}(\theta)$ can be measured experimentally. For all these cases the $(P_\gamma)_0$ quantity essentially describes the PNC effect. In all the above formulas θ represents the angle between the emitted photon and the axis of polarization (if any).

5.1. Parity-mixed doublets in ^{18}F

In the excitation spectrum[64] of the ^{18}F nucleus there are two PMDs (see Table I): one at 1.0 MeV ($\Delta E \approx 40$ keV) and another at 6.8 MeV ($\Delta E \approx 4$ keV) excitation energy. The difference between the two PMDs is that PMD1 is of the isovector type and can be investigated via the circular polarization of the γ rays, while PMD2 cannot be interpreted yet, whether it is of the isoscalar or of the isovector type, because the isospins are not experimentally known; however, it is a very favorable ($F=130000$; see Table I) case for studying the structure of the weak hadron–hadron interaction via the $(\vec{p},p)$ resonance scattering or $(\vec{p},\alpha)$ resonance reaction.

We want to discuss the first PMD case in somewhat more detail, since it has been the object of considerable experimantal and theoretical work. Let us denote the upper state (1.08054 MeV) (see Table I) by $|a\rangle$ and the lower one (1.041155 MeV) by $|b\rangle$. The γ decay of the state $|a\rangle$ to the ground state ($J^\pi T = 1^+0$) includes a parity-conserving (PC) E1 transition and a PNC M1 transition. The circular polarization can be expressed as follows:

$$P_\gamma = 2f\frac{M_{\rm PNC}}{\Delta E}, \tag{48}$$

where the ratio f of the reduced matrix elements for the regular decays of the members of the doublet can be deduced (apart from the sign) from the known lifetimes[64] and energies:

$$f = \frac{m_1}{e_1} = \sqrt{\frac{E_a^3\tau_a}{E_b^3\tau_b}} \approx 112. \tag{49}$$

The PMD lifetimes are in the relation $\tau_a(27.5\pm 1.9\ \text{ps}) \gg \tau_b(2.55\pm 0.45\ \text{fs})$, because isospin selection rules forbid the E1 ($\Delta T=0$) transition, but not the M1 ($\Delta T=1$) transition. The circular polarization is therefore two orders of

magnitude larger than the PNC admixture coefficient $M_{PNC}/\Delta E$. This is a good example of amplification of the PNC effect, due to the nuclear structure. The M1 transition from the state $|b\rangle$ to the ground state is one of the strongest known M1 transitions (10.3±1.5 W.u.), which further justifies the two-level mixing approximation.

The experimental results are:

Caltech–Seattle[49]	1979	$P_\gamma=(-0.7\pm2.0)\cdot10^{-3}$
Florence[52]	1980	$P_\gamma=(-0.4\pm3.0)\cdot10^{-3}$
Mainz[53]	1982	$P_\gamma=(-1.0\pm1.8)\cdot10^{-3}$
Bini[51]	1982	$P_\gamma=(0.2\pm0.6)\cdot10^{-3}$
Queens Univ.[50]	1982	$P_\gamma=(0.15\pm0.55)\cdot10^{-3}$

If one takes into account the analyzing power (≃0.02) of the Compton polarimeters, this would require a precision $\simeq1.2\cdot10^{-5}$ in the counting asymmetry, and it might be difficult to maintain the systematic errors below this limit. The real value of the circular polarization mentioned above could be some units above 10^{-5} if we consider the chiral-soliton approach[15] and hence difficult to measure exactly. This PMD1 case in ^{18}F could be considered a good example for the importance of the PNC matrix element given by the nuclear-model calculations in the first predictions of favorable cases. The theoretical value of 0.37 eV (Ref. 16) comes out to be too large. More sophisticated shell-model calculations[43] show a decrease of the value of the PNC matrix element with increase of the number of valence orbitals, in agreement with experimental suggestions; however, no convergence seems to appear.

5.2. Parity-mixed doublets in ^{19}F

We consider, however, the only good experiments with light nuclei that concern the asymmetry A_γ in the 110-keV γ-ray emission of ^{19}F with respect to the direction of the spin of the $(1/2)^-$ 110-keV state, which is produced with large polarization by the reaction ^{22}Ne$(\vec{p},\alpha)^{19}$F. In the particular case of a $(1/2)^-\rightarrow(1/2)^+$ transition, $A_\gamma=A_\gamma^{(1)}\cdot p((1/2)^-)$, where $p((1/2)^-)$ is the polarization fraction of the parent state and the asymmetry $A_\gamma^{(1)}$ for total polarization has the same numerical value as the circular polarization P_γ.

The experimental results are:

Seattle[18]	1982	$A_\gamma^{(1)}=(-8.5\pm2.6)\cdot10^{-5}$
Zurich[19]	1982	$A_\gamma^{(1)}=(-4.5\pm3.6)\cdot10^{-5}$

The theoretical value of the circular polarization can be obtained from the formula

$$P_\gamma=2\frac{M_{PNC}}{\Delta E}\frac{\mu_1^{(1/2)^-}-\mu_1^{(1/2)^+}}{\langle(\frac{1}{2})^-|E_1|(\frac{1}{2})^+\rangle}, \tag{50}$$

in which the reduced matrix element of the irregular M1 transition depends on the difference of the static magnetic dipole moments in the ground and the first excited state of ^{19}F. The former is known, $\mu((1/2)^-)=2.628$ n.m. (Ref. 64), while the latter can be calculated with reasonable accuracy[18,24,135] and comes out to be small, $\mu((1/2)^+)=-0.2$ n.m. From the lifetime $\tau=853\pm10$ ps of the 110-keV level[64] we can estimate the E1 matrix element, and the small enhancement factor comes out to be $f\simeq11$. The circular polarization can then be obtained as $(-8.9\pm1.6)\cdot10^{-5}$, using $M_{PNC}=0.46$ eV,[16] in good agreement with experiment.

5.3. Parity-mixed doublet in ^{21}Ne

One of the best supports for the DDH "best" values comes from the study of the parity violation in the transition $1/2^-$, $T=1/2$ (2.789 MeV)$\rightarrow3/2^+$, $T=1/2$ (g.s.) in ^{21}Ne. According to the analysis made by Millener *et al.*[27] and subsequently by Haxton *et al.*,[24] the effect should be determined *a priori* by the strength of the neutron–nucleus weak force for its largest part. With the DDH "best" values of the meson–nucleon weak coupling constants, this strength is expected to be small, in agreement with the experimental absence of an effect in this process. Said differently, the isoscalar and isovector contributions of the nucleon–nucleus weak force, which add to each other in ^{19}F, would cancel in ^{21}Ne. This, however, presupposes a sizable isovector contribution, which is not seen in ^{18}F at the expected level: something must be wrong.

While the accuracy of estimations of the PNC effects in light nuclei is not as good as originally expected, one has in both ^{18}F and ^{19}F some check of the relevant nuclear structure by looking at the β decay of ^{18}Ne and ^{19}Ne, respectively, which involve an operator, $\vec{\sigma}\cdot\vec{p}$, very close to the one determining PNC effects in complex nuclei in the single-particle approximation.[136] There is no possible similar check in ^{21}Ne. Only comparison of the different calculations can provide some information on the reliability of the estimates. While the studies by Millener *et al.*[27] and Haxton *et al.*[24] agree qualitatively on the fact that nuclear structure favors the contribution of the PNC neutron–nucleus force, a quite different conclusion was drawn by Brandenburg *et al.*[28] From a comparison of results with different strong-interaction models, they concluded that the isovector contribution, whose sign was changing with the model, is very sensitive to the description of the nucleus. In the meantime, this isoscalar contribution was changing by more than an order of magnitude. In this paper, we reexamine these claims on the basis of new calculations including the nuclear models that they used. Our conclusion is opposite to theirs. The isovector contribution is well determined in sign, while the isoscalar one is not. In particular, this last contribution may be negligible. In such a case the parity nonconservation in the transition $1/2^-$, $T=1/2$ (2.789 MeV)$\rightarrow3/2^+$, $T=1/2$ (g.s.) in ^{21}Ne would be a process sensitive to the isovector part of the weak force, as in the transition 0^-, $T=0$ (1.08 MeV)$\rightarrow1^+$, $T=0$ (g.s.) in ^{18}F, and the absence of an effect at the expected level in ^{21}Ne could be usefully correlated with that in ^{18}F.

The circular polarization of photons emitted in the transition $1/2^-$, $T=1/2$ (2.789 MeV)$\rightarrow3/2^+$, $T=1/2$ (g.s.) in ^{21}Ne is expected to be dominated by the contribution from the parity admixture of the $1/2^-$, $T=1/2$ state at 2.789 MeV with the $1/2^+$, $T=1/2$ state at 2.796 MeV. The relation of the circular polarization P_γ to the PNC matrix element $\langle1/2^-,T=1/2\ (2.789\ \text{MeV})|H_{PNC}|1/2^+,T=1/2\ (2.796\ \text{MeV})\rangle$ is given by

TABLE VI. Values of the matrix elements $M_{k,s}^{(\Delta T)}$ for different descriptions of the nucleus (in units of MeV). In the first column, the matrix elements are given. The next columns contain results corresponding to models whose description is given in the text. The results corresponding to the oversimplified model in which the states $1/2^+$ and $1/2^-$ are described by one neutron occupying, respectively, the $2s_{1/2}$ and $1p_{1/2}$ orbits (with a ^{12}C core) are given in the sixth column. The last column gives the dominant character of the transition for the component under consideration. For each component the contribution corresponding to the ^{12}C core is given in the first row, while the second row incorporates the contribution of the valence nucleons.

Coupling element	ZBMMI	ZWM (Z)	REWIL (F)	ZBMII	Valence neutron (^{12}C)	Matrix transition
$M_{0,\pi}^{(1)}$	0.1884	0.1579	0.2310	0.2592	0.733	$(^3S_1-^3P_1)$
	0.2092	0.1657	0.2557	0.2967		
$M_{0,\rho'}^{(1)}$	0.0116	0.0097	0.0142	0.0159	0.0451	$(^3S_1-^3P_1)$
	0.0146	0.0114	0.0174	0.0203		
$M_{1,\rho}^{(1)}$	0.0092	0.0077	0.0113	0.0127	0.0358	$(^3S_1-^3P_1)$
	0.0127	0.0101	0.0151	0.0174		
$M_{2,\rho}^{(1)}$	0.0116	0.0097	0.0142	0.0159	0.0451	$(^1S_0-^3P_0)$
	0.0065	0.0059	0.0123	0.0142		
$M_{3,\rho}^{(1)}$	0.0098	0.0082	0.0120	0.0134	0.0380	$(^1S_0-^3P_0)$
	0.0071	0.0064	0.0120	0.0137		
$M_{1,\omega}^{(1)}$	0.0086	0.0072	0.0106	0.0119	0.0336	$(^3S_1-^3P_1)$
	0.0146	0.0095	0.0142	0.0163		
$M_{2,\omega}^{(1)}$	0.0110	0.0092	0.0135	0.0151	0.0427	$(^1S_0-^3P_0)$
	0.0061	0.0056	0.0116	0.0135		
$M_{3,\omega}^{(1)}$	0.0091	0.0077	0.0112	0.0126	0.0356	$(^1S_0-^3P_0)$
	0.0067	0.0060	0.0112	0.0128		
$M_{4,\rho}^{(0)}$	0.0077	0.0002	0.0083	−0.0112	−0.0676	$-\frac{3(^1S_0-^3P_0)+3(^3S_1-^1P_1)}{4}$
	0.0153	0.0032	−0.0083	−0.0105		
$M_{5,\rho}^{(0)}$	0.0004	0.0000	−0.0004	−0.0005		$-\frac{3(^1S_0-^3P_0)-3(^3S_1-^1P_1)}{4}$
	0.0045	0.0040	0.0034	0.0041		
$M_{6,\omega}^{(0)}$	0.0024	0.0001	−0.0026	−0.0035	−0.0213	$-\frac{3(^1S_0-^3P_0)-(^3S_1-^1P_1)}{4}$
	0.0087	0.0047	0.0009	0.0010		
$M_{7,\omega}^{(0)}$	0.0040	0.0001	−0.0042	−0.0057	−0.0346	$-\frac{3(^1S_0-^3P_0)+(^3S_1-^1P_1)}{4}$
	0.0093	0.0030	−0.0033	−0.0045		

$$|P_\gamma(2.789\ \text{MeV})| = \left(10.5 \pm \frac{0.7}{2.8}\right) 10^{-2}\ \text{eV}^{-1},$$

$$|\langle \tfrac{1}{2}^-, T=\tfrac{1}{2}\ (2.789\ \text{MeV})|H_{\text{PNC}}|\tfrac{1}{2}^+, T=\tfrac{1}{2}\ (2.796\ \text{MeV})\rangle|. \tag{51}$$

The calculation of the weak matrix element has been performed with the standard PNC potential arising from the exchange of π, ρ, and ω mesons, together with various descriptions of the effective NN interaction.

We present in Table VI the details of the contributions of the different components of the PNC potential to the PNC matrix element $\langle \frac{1}{2}^-,\ T=1/2\ (2.789\ \text{MeV})|H_{\text{PNC}}|1/2^+,\ T=1/2\ (2.796\ \text{MeV})\rangle$. To facilitate the comparison, we do not introduce the coupling constants, so that what is given represents the raw matrix elements

$$M_{k,s}^{(\Delta T)} = \langle \tfrac{1}{2}^-,\ T=\tfrac{1}{2}\ (2.789\ \text{MeV})|f_{k,s}^{(\Delta T)}|\tfrac{1}{2}^+,$$
$$T=\tfrac{1}{2}\ (2.796\ \text{MeV})\rangle, \tag{52}$$

where the operators $f_{k,s}^{(\Delta T)}$ are defined by Eqs. (8). For each of them, besides the total contribution, we give the separate contribution of the core, presently built by filling its orbits $1s_{1/2}$ and $1p_{3/2}$. It corresponds in the present case to a single-particle transition involving nucleons in orbits $1p_{1/2}$ and $2s_{1/2}$. As a benchmark, we also give the result corresponding to a pure case, where the $1/2^-$ and $1/2^+$ states would be considered as made of one neutron moving in the field of an inert core (^{12}C) and occupying, respectively, the above orbits $1p_{1/2}$ and $2s_{1/2}$. The comparison with the full calculations may give evidence for specific nuclear-structure effects such as depopulation of these single-particle states, pairing, and possible departures from the single-particle approximation, together with some suppression or enhancement of particular contributions of the weak force. In reporting the results for various strong-interaction models, we paid particular attention to the intrinsic sign of the weak matrix element $\langle 1/2^-,\ T=1/2\ (2.789\ \text{MeV})|H_{\text{PNC}}|1/2^+,\ T=1/2\ (2.796\ \text{MeV})\rangle$. Obviously, this sign is not measurable, since it depends on the sign conventions used to describe the states $|1/2^-,\ T=1/2\ (2.789\ \text{MeV})\rangle$ and $|1/2^+,\ T=1/2\ (2.796\ \text{MeV})\rangle$. However, the comparison of the signs obtained with different strong-interaction models may be relevant, and some change may indicate a strong sensitivity to particular features of the nuclear description. We therefore carefully examined these results. The task is not *a priori* straightforward. One may imagine, for instance, that the sign of the isovector contribution is not settled, as stated by Brandenburg *et al.*,[28] while the sign of the isoscalar contribution would be well determined, or vice versa. For the strong-interaction models used here, we found that the signs of the largest contribution (at the level of the two-body matrix elements) were the same up to a common phase, leaving no doubt as to the origin of a difference in sign in the results coming from the computer. The results presented in Table VI have been corrected so that

the dominant individual contributions are the same. Differences in sign between some of these results therefore reflect differences in the physical description of the nucleus.

Owing to the short range of the operators entering into H_{PNC}, the estimates of its matrix elements are expected to be very sensitive to short-range correlations. To take them into account, we introduced in the calculations the correlation function of Miller and Spencer,[65] for the even as well as the odd parity components (see Sec. 3.1).

The microscopic structure of the nuclear levels of the parity-mixed doublet has been obtained by using the OXBASH code in the Michigan State University version,[63] which includes different model spaces and different effective two-nucleon interactions.

In these calculations the ZBM model space and the interactions ZBMI, ZBMII, ZWM, and REWIL have been used (see Sec. 3).

The comparison with the predictions of the PNC single-particle model (column labeled "valence nucleon" in Table VI) shows that the core contribution is suppressed by a factor 3–4 for the isovector part. For some part, this factor arises from the fact that the $1/2^+$ states and $1/2^-$ states are not described by pure configurations with a neutron in $2s_{1/2}$ and $1p_{1/2}$ orbits, respectively. For the other part, it represents a pairing effect, which, for the type of operator considered here, is usually included by a factor $u_i u_f - v_i v_f$. Indeed, the dominant PNC contribution due to the transition $2s_{1/2} \leftrightarrow 1p_{1/2}$ is canceled for $\simeq$20–30% by the similar, but time-reversed, transition $1\bar{p}_{1/2} \leftrightarrow 2\bar{s}_{1/2}$.

The situation is somewhat similar for the isoscalar contribution, but the pairing effect is much more pronounced, since the contribution of the second transition, $1\bar{p}_{1/2} \leftrightarrow 2\bar{s}_{1/2}$, becomes comparable to the first one, and even larger in some cases, giving rise either to a complete cancellation (ZWM) or to a change in sign in other cases (ZBMI). The relative weights of these two contributions have been retained in classifying the different models in Table VI, those on the left favoring a proton transition, and those on the right favoring a neutron transition. In between, there is a possibility of a total absence of the isoscalar contribution (ZWM), the isovector contribution being relatively stable and varying by a factor of 1.5 at most.

The examination of the contribution of the valence nucleons ($1p_{1/2}$,$1d_{5/2}$,$2s_{1/2}$) is also instructive. As all core nucleons generally contribute coherently to the single-particle PNC interaction, one might expect *a priori* that they would increase the core contribution. Table VI shows that this is true in many cases, for the transition $^3S_1 - {}^3P_1$ as well as for the transition $^3S_1 - {}^1P_1$ (after appropriately separating in this case the contributions arising from the transitions $^3S_1 - {}^1P_1$ and $^1S_0 - {}^3P_0$ assumed to dominate). This is not so, however, for the isovector $^1S_0 - {}^3P_0$ transition, whose contribution is small (ZBMII) or even destructive (ZBMI). For the isoscalar $^1S_0 - {}^3P_0$ transition the situation is much more contrasted (decrease for ZBMII and increase for ZBMI, for absolute values), but algebraically the effect always goes in the same direction. Clearly, the results are very sensitive to strong interactions in the $^1S_0$ and $^3S_1$ states, whose relative strengths in nuclei are not well determined (see some discussions in Ref. 141 and some other references therein). The well known pairing correlations between like particles tend to support the dominance of the first one, whereas the existence of the deuteron as a bound state in the $^3S_1$ channel indicates that the corresponding force should have the most important role. As for the core contribution, the dependence of the results on the transition can be traced back to specific "pairing" effects and to a more or less destructive interference of the contributions of the single-particle transitions $2s_{1/2} - 1p_{1/2}$ and the time-reversed ones $1p_{1/2} - 2s_{1/2}$.

The large variation of the isoscalar contribution with the strong-interaction model makes it useful to present a few simple pictures which may occur. Checking how well they are realized in actual results is not easy, and they are given as guidelines for future research. The first picture presupposes that the $1/2^+$ state is given by one neutron in the valence orbit $2s_{1/2}$, moving in the field of a core (^{20}Ne), whose $1p_{1/2}$ shell is not completely filled. In the single-particle approximation, the PNC transition from the state $1/2^+$ to the state $1/2^-$ occurs via a transition from the $2s_{1/2}$ neutron orbit to the $1p_{1/2}$ orbit. It is a particle-like transition. This picture seems appropriate to describe results obtained with the ZBMII and REWIL models.

The other schematic pictures are inspired by the Nilsson model and presuppose some relationship between the parity doublets considered here and the one in ^{19}F, where parity nonconservation gives evidences for the character of a proton–hole-like transition. The parity doublet in ^{21}Ne might be obtained by creating holes in the deformed orbits $[220]1/2^+$ and $[101]1/2^-$ of ^{20}Ne, to which two inert nucleons in the orbit $[221]3/2^+$ would be added. Two extreme possibilities occur, depending on whether this pair is in the $T=1$ or $T=0$ state. The first one, where the hole is coupled to the $T=1$ pair, so that the total isospin is $T=1/2$, gives rise to a result where contributions of the neutron and proton single-particle PNC interactions are in the ratio 2:1, corresponding to the ratio of isovector and isoscalar contributions, $-1{:}3$. This picture, which apparently underlies the results of Millener *et al.*,[27] where the role of the neutron transition is somewhat enhanced (the above ratios are, respectively, 3.7:1 and $-1{:}1.73$), has no counterpart here. As mentioned above, the results for ZBMII, which favor a neutron PNC transition, correspond to a particle transition and not to a hole one, as in the calculations of Millener *et al.*[27] To get it, the sign of the "pairing" effect for the isovector contribution should change, as it does for the isoscalar contribution. While the present calculations give evidence for a well determined sign for the isovector contribution, it may be that the change in sign observed for the contribution of valence nucleons in some cases (isovector transition $^1S_0 - {}^3P_0$) is an indication that the picture underlying the results of Millener *et al.* is not completely absent from the present results.

Some nuclear aspects of the calculations presented here have already been discussed. Further comments may be in order, especially in relation to other studies. Apart from the sign of the isovector contribution that we discussed at length above, we essentially agree with the results of Brandenburg *et al.*,[28] whose models Z and F correspond to the models denoted here by ZWM and REWIL. The large sensitivity to

the nuclear model of these results for the isoscalar contribution, apparently unnoticed, is further confirmed by the present results for the models ZBMI and ZBMII. The results of Millener *et al.*[27] were obtained with a single-particle PNC interaction (const $\vec{\sigma}\cdot p$). For many transitions involving low-energy states, this approximation, possibly corrected for the finite range of the nucleus, has been able to reproduce the essential features of more elaborate calculations involving two-body forces (see, for instance, Ref. 138 and references therein). It is interesting to notice that the improved calculations by Adelberger *et al.*[16] for ^{18}F, ^{19}F, and ^{21}Ne give evidence for a single-particle transition character, while the description of these nuclei already reveals a complicated structure. In the results presented here, the above approximation still works, but in the range where the core contribution is the dominant one. Unlike ^{19}F, however, relatively large departures appear, especially for ZBMI, where the valence-nucleon contribution gives an increase in some cases [a factor 2 for the component $g_\rho h_\rho^0(1+\mu_v)$], and a decrease in other cases [a factor 1.8 for the component $g_\rho h_\rho^1(1+\mu_v)$]. This is perhaps an indication that ^{21}Ne is in some transition region, making it more difficult to obtain well-defined predictions. Further support for this statement comes from the character of the hole transition of the results of Millener *et al.* and Adelberger *et al.*, which is confirmed here only for the isoscalar contribution (ZBMI and ZWM). Their approach necessarily implies such a structure, since they allow for only one hole in the $1p_{1/2}$ shell. The absence of a restriction in this respect in the present calculations leads to a quite different picture, since the isovector contribution is uniformly of the particle type of transition. In view of this, the above approximation appears to be a poor one. This does not mean that the present results are free from criticism. Studies in ^{18}F and ^{19}F show that some suppression of the PNC effect occurs, owing to the deformation of the nucleus, whose inclusion requires that the particles in the $1p_{3/2}$, $1d_{3/2}$, and $1f_{5/2}$ shells be the active ones (besides the particles in the $p_{1/2}$, $1d_{5/2}$ and $2s_{1/2}$ shells). The possible transitional character of ^{21}Ne precludes a statement as to the precise role of these corrections, but a provisional suppression factor of 3, as in ^{18}F and ^{19}F, seems quite reasonable. This should be borne in mind when making the comparison with experiment.

After discussing some features relevant to the nuclear description itself, it may be appropriate to consider those related to the weak interaction. The differences between the ρ and ω exchange contributions reflect the differences used for the meson masses. Their ratio for terms having the same spin–isospin structure is roughly given by the factor m_ρ^2/m_ω^2 ($\simeq$0.965 here), corrected for the effect of short-range correlations, which tend to decrease it. For isoscalar contributions, this feature is more difficult to check, owing to a difficult isospin structure. As to the short-range correlations, one would expect that the difference between the contributions of the commutator and anticommutator terms in the PNC potential reflects the fact that the one for a valence neutron (column 6 of Table VI) is dominated by S and P NN transitions. The suppression of some contributions partly invalidates the argument, especially for those dominated by the $^1S_0$–$^3P_1$ transition, where the P to D transitions acquire a relatively larger weight. These last transitions are quite sensitive to the longer-range description of ρ and ω exchanges, due, for instance, to the coupling of the ρ to the 2π continuum.[139] Their mirror role suggests that we forget them at the present stage of studies of PNC effects. Table VI can thus be considerably simplified, to be expressed in terms of four elementary amplitudes:[137] $\bar{\nu}_0^0$ and $\bar{\nu}_1^1$ ($^1S_0$–$^3P_0$, isoscalar and isovector), $\bar{u}$ ($^3S_1$–$^1P_1$, isoscalar), and $\bar{w}$ ($^3S_1$–$^3P_1$, isovector), where

$$M^2\bar{v}^{0,1}=-(g_\omega h_\omega^{(0,1)}+g_\rho h_\rho^{(0,1)})\frac{M^2}{4\pi m_\rho^2}\cdot 0.23-[g_\omega h_\omega^{(0,1)}(1+\mu_s)+g_\rho h_\rho^{(0,1)}(1+\mu_v)]\frac{M^2}{4\pi m_\rho^2}\cdot 0.27, \tag{53}$$

$$M^2\bar{u}=-(g_\omega h_\omega^{(0)}-3g_\rho h_\rho^{(0)})\frac{M^2}{4\pi m_\rho^2}\cdot 0.23-[-g_\omega h_\omega^{(0,1)}(1+\mu_s)+3g_\rho h_\rho^{(0,1)}(1+\mu_v)]\frac{M^2}{4\pi m_\rho^2}\cdot 0.27, \tag{54}$$

$$M^2\bar{w}=-(g_\omega h_\omega^{(1)}+g_\rho h_\rho^{(1)})\frac{M^2}{4\pi m_\rho^2}\cdot 0.23-g_\rho h_{\rho'}^{(1)}\frac{M^2}{4\pi m_\rho^2}\cdot 0.27+\frac{1}{\sqrt{2}}g_\pi h_\pi^{(1)}\frac{M^2}{4\pi m_\pi^2}\cdot 0.11. \tag{55}$$

The factors 0.23, 0.27, and 0.11 incorporate the effect of both the range (important for the π exchange case) and short-range correlations. They may be changed according to the model of short-range correlations. For simplicity, we neglected the mass differences between the ρ and ω mesons. In the case of π exchange, the factor has been partly estimated in nuclear matter and incorporates the contribution of the transitions P–D, D–F, whose destructive role may be smaller in light nuclei, thus enhancing the π exchange contribution with respect to this estimate by 15–25%. The results are presented in Table VII. The advantage of the above amplitudes is to facilitate the incorporation in the first approximation of new physical inputs dealing with the short-range PNC-NN interaction (short-range correlations, tensor coupling between the $^3S_1$ and $^3D_1$ components, other meson exchange, hadronic form factor) without repeating all the calculations.

Further simplification is obtained by using the strengths of the proton and neutron PNC forces:

$$X_N^p=M^2(\tfrac{1}{2}\bar{u}+\tfrac{3}{2}\bar{v}^0+\bar{v}^1+\bar{w}), \tag{56}$$

$$X_N^n=M^2(\tfrac{1}{2}\bar{u}+\tfrac{3}{2}\bar{v}^0-\bar{v}^1-\bar{w}). \tag{57}$$

As mentioned previously, these quantities, which have been used in analyzing various PNC effects in complex nuclei,[137] may not be so good to represent the PNC effect in ^{21}Ne. They are nevertheless useful to see at a glance the dominant character of some matrix element: a neutron or proton transition. Expressions in terms of them are also given in Table VII.

In the comparison with experiment, we retain the following features revealed by the estimates. The estimate of the

TABLE VII. Expressions for the matrix element $\langle 1/2^-, T=1/2\ (2.789\ \text{MeV})|\ H_{\text{PNC}}|1/2^+, T=1/2\ (2.796\ \text{MeV})\rangle$ in terms of the $S-P$ transition amplitudes as defined in Ref. 137 ($\bar{w}$ for ${}^3S_1-{}^3P_1$, $\Delta T=1$; $\bar{v}^1$ for ${}^1S_0-{}^3P_0$, $\Delta T=1$; $\bar{u}$ for ${}^3S_1-{}^3P_1$, $\Delta T=0$; and $\bar{v}^0$ for ${}^1S_0-{}^3P_0$, $\Delta T=0$; as well as in terms of the strengths of the proton–nucleus and neutron–nucleus PNC forces (in units of MeV). As in Table VI, the first row corresponds to a ^{12}C closed core, while the second row incorporates the contribution of valence nucleons. The above results obviously imply approximations such as neglect of contributions from $P-D$ transitions.

	Kuo (Ref. 72)	ZBMI	ZWM	REWIL	ZBMII	Valence neutron
$M^2\bar{w}$		0.174	0.146	0.214	0.240	0.68
		0.228	0.179	0.272	0.316	
$M^2\bar{v}^1$		0.179	0.150	0.219	0.246	0.70
		0.114	0.104	0.203	0.234	
$M^2\bar{u}$		0.074	0.002	−0.080	−0.100	−0.68
		0.087	−0.022	−0.135	−0.171	
$M^2\bar{v}^0$		0.080	0.002	−0.089	−0.114	−0.68
		0.216	0.089	−0.035	−0.050	
$\frac{X_N^p-X_N^n}{2}$	−0.19	0.177	0.148	0.217	0.243	0.69
		0.172	0.141	0.237	0.275	
$\frac{X_N^p+X_N^n}{2}$	0.24	0.077	0.002	−0.084	−0.107	−0.69
		0.151	0.033	−0.085	−0.110	
X_N^p	0.02	0.127	0.075	0.066	0.068	0.
		0.161	0.087	0.076	0.082	
X_N^n	0.22	−0.050	−0.073	−0.150	−0.175	−0.69
		−0.010	−0.054	−0.161	−0.192	

nuclear part of the isovector contribution is rather well determined. The isoscalar one, including its sign, is uncertain and has a weight rather disfavored in comparison with the isovector one (see Table VII). From the comparison of similar calculations with β decay in ^{18}F and ^{19}F, an overall suppression by a factor 3 is quite likely, but it should be borne in mind that the nuclear uncertainty here may result in an effect more complicated than such a factor.

The circular polarization of γ emitted in the transition $1/2^-$, $T=1/2$ (2.789 MeV)$\rightarrow 3/2^+$, $T=1/2$ (g.s.) in ^{21}Ne has been measured as[26]

$$P_\gamma=(0.8\pm 1.4)\cdot 10^{-3}. \tag{58}$$

The error is large, but in fact it provides an upper limit, which appears to be quite restrictive. Combining the results of Table VI with the coupling constants given in Table III ("best" values of DDH), and using the relation of P_γ to the PNC matrix element $\langle 1/2^-, T=1/2\ (2.789\ \text{MeV})|H_{\text{PNC}}|1/2^+, T=1/2\ (2.796\ \text{MeV})\rangle$, we find that many of the individual contributions exceed the experimental upper limit, or just reach it. Allowance for a possible overestimate by a factor 3 leaves two contributions which may be of some relevance: the π-exchange and the isoscalar ρ-exchange ones [respectively, $(10–20)\cdot 10^{-3}$ and $(-5.8)\cdot 10^{-3}$].

While the isovector contribution to P_γ agrees in size (but not necessarily in sign) with that obtained under similar conditions by Adelberger *et al.* $(12\cdot 10^{-3})$, the isoscalar one is smaller than theirs $(-12\cdot 10^{-3})$. The nice cancellation between the isovector and isoscalar contributions in their results, which made them consistent with the upper limit on P_γ, no longer holds.

Examination of the present results shows that the cancellation is not always present (ZBMI) and that, in cases where there is some, the relative ratio of the π and ρ exchange contributions expected from the DDH "best" values has to be changed significantly. Fixing the isoscalar ρNN coupling at its "best" DDH value, in agreement with observations of PNC effects in pp scattering at low energy (15 MeV and 45 MeV), implies that the corresponding πNN coupling constant must be reduced by a factor of 3 in order to match the experimental upper bound on P_γ. The resulting value (REWIL, ZBMII), $h_\pi^{(1)}=0.15\cdot 10^{-6}$, would be quite compatible with the limit obtained from the upper bound on the PNC effect in the transition 0^- (1.08 MeV)$\rightarrow 1^+$ (g.s.) in ^{18}F ($|h_\pi^{(1)}|<0.15\cdot 10^{-6}$). Thus, far from supporting the "best" values of DDH, the PNC in ^{21}Ne would add to that in ^{18}F, to favor a value of $h_\pi^{(1)}$ significantly smaller than the DDH "best" value.

In discussing PNC effects in nuclei, the effect of the tensor force which admixes the ${}^3D_1$ component with the ${}^3S_1$ state, is generally neglected. Its role is twofold here and tends to provide further support for lower values of $h_\pi^{(1)}$. In the case of π exchange, it leads to an enhancement of the contribution of the ${}^3S_1-{}^3P_1$ transition, which compensates a large part of the effect of the short-range repulsion at short distances.[137] The actual value of $h_\pi^{(1)}$, which may be extracted from a comparison of measurements with a theoretical estimate that is more elaborate in the above respect, should be accordingly corrected downwards. This statement is quite general and also applies to conclusions drawn from the study of PNC in ^{18}F.[16]

The important role of tensor correlations for the ρ-exchange contribution is somewhat specific to some of the present results for ^{21}Ne (REWIL, ZBMII). As can be seen from Table VII, the isoscalar contribution for those cases is dominated by the ${}^3S_1-{}^1P_1$ transition. Tensor correlations may reduce it by a factor 3–4 (Reid soft-core case), making the total isoscalar contribution smaller. This requires a lower value of the isovector contribution, and therefore a lower value of $h_\pi^{(1)}$, so that the destructive sum of the isoscalar and

TABLE VIII. Detailed contributions to the coupling constants $h_\pi^{(1)}$ in the DDH scheme as completed in Ref. 142. Results are given for different values of the factor K (Refs. 13 and 142) which accounts for the effect of strong interactions.[137] Three types of contributions are included: sum rule (related to the charged-current contribution), PNC in the wave function, and factorization. The results for later comparison are denoted by the initials of the authors. Some earlier results by Weinberg,[4] Gari and Reid,[140] or Khatsimovsky[62] would enter in the column labeled We ($K\to\infty$), Ga ($K=0$), or Kh, respectively. Contributions by Kaiser and Meissner[15] or Dubovik and Zenkin[14] would enter in the rows labeled KM or DZ, respectively. Contributions involving the (colored) strange content are given in the first two columns. The factor f_π^c has the value $f_\pi^c=0.38\cdot10^{-7}$.

		Sum rule $\bar{s}s$..	PNC factorization in the w.f.	
$K=1$	$h_\pi^{(1)}=f_\pi^c\cdot($	1+0.−3.3	+2.1 +1.3)	$=0.4\cdot10^{-7}$
			...K.M. ...	$=0.4\cdot10^{-7}$
$K=4$	$h_\pi^{(1)}=f_\pi^c\cdot($	1+4.6−3.5	+0.1 +4.3)	$=2.5\cdot10^{-7}$
			...D.Z. ...	$=0.4\cdot10^{-7}$
$K=7$	$h_\pi^{(1)}=f_\pi^c\cdot($	1+6.0−4.3	−0.5 +7.0)	$=3.5\cdot10^{-7}$
	$f_\pi^c=0.38\cdot10^{-7}$	We Ga	Kh	

isovector contributions still matches the upper limit on the circular polarization P_γ.

At this point, it may be appropriate to recall a few predictions for $h_\pi^{(1)}$. In this order, the DDH approach is quite useful, as it provides a general scheme, where many contributions considered in the literature can be accommodated quite easily. Results are given in Table VIII for different values of the factor K ($K=1,4,7$) defined in Refs. 13 and 142, which characterizes the strong-interaction effects. Partial contributions are also exhibited. They correspond to the sum-rule contribution (related in one way or another to the charged-current contribution), to the parity violation in the wave function, and to the factorization approximation. Earlier contributions calculated by Weinberg[4] or Gari and Reid[140] would enter in the column indicated by We and Ga, respectively. Later contributions by Dubovik and Zenkin,[14] Kaiser and Meissner,[15] or Khatsimovsky[62] can be regarded as particular cases of DDH expectations. In spite of somewhat different approaches in some cases, they compare well with them. The corresponding contributions in the DDH scheme are underlined in Table VIII (respectively, labeled by KM, DZ, and Kh). Contributions involving a (colored) strange content are given in the two first columns, where the first one corresponds to the charged-current part of the weak interaction.

As can be seen from Table VIII, small values of $h_\pi^{(1)}$ are found for small values of the factor K or/and in the absence of strange content in the nucleon. This might represent a great achievement of studies of PNC effects in nuclear forces. However, it is difficult to neglect the strange content of the nucleon at the present time, as it appears to play some role in different places,[141] or to imagine that strong-interaction effects ($K\neq1$) are totally absent. It is more probable that the explanation of a low value of $h_\pi^{(1)}$ is to be found in the incompleteness of the estimates. Owing to a lack of information, and because it was considered a second-order effect in gluon exchange, the contribution of an uncolored strange component $\bar{s}s$ in the nucleon has not been incorporated in the estimates by DDH. As was noted in Ref. 140, such a contribution could be enhanced by the presence of a large overall factor in the effective weak interaction. On the other hand, this effective interaction only contains the dominant terms. Other ones may play some non-negligible role in estimating the coupling constant $h_\pi^{(1)}$.

We reexamined estimates of the circular polarization of γ rays emitted in the transition $1/2^-$, $T=1/2$ (2.789 MeV)$\to3/2^+$, $T=1/2$ (g.s.) in ^{21}Ne, which involves the parity admixture of two closed states $1/2^-$, $T=1/2$ (2.789 MeV) and $1/2^+$, $T=1/2$ (2.796 MeV). New estimates have been added to previous ones. From the study a different interpretation of the measurement is suggested. In contrast to the previous claim by Brandenburg *et al.*,[28] we found that the isovector contribution is well defined in sign, while the isoscalar contribution is not and is somewhat disfavored. This conclusion agrees with the recent result of Ref. 43 based on a much larger valence basis. Our conclusion is based on a careful examination of the sign of the dominant individual contribution. Such a procedure allows us to reduce the ambiguity to an overall sign that tends to appear at random from the computer in calculating the wave functions. The difference with respect to Adelberger *et al.*[16] appears to be due to the quite understandable restriction of their calculation to one hole at most in $p_{1/2}$. Qualitatively, it looks as if the total result would be the sum of two different contributions, which, in a deformed single-particle basis, would imply the transition $[220]1/2^+\to[101]1/2^-$ (dominant in ^{18}F and ^{19}F) and a transition implying the $1/2^+$ orbit ($[211]1/2^+$), such that the PNC matrix element would have the form

$$\langle V_{\rm PNC}\rangle\simeq\beta^2\left(\frac{X_N^n+X_N^p}{2}+\frac{X_N^n-X_N^p}{2}\right)$$
$$-\alpha^2\left(\frac{X_N^n+X_N^p}{2}+\frac{1}{3}\cdot\frac{X_N^n-X_N^p}{2}\right). \qquad (59)$$

The first contribution would have mainly a particle-type character, while the second one would be a hole-type transition. By varying continuously the ratio of these two contributions, one would go from results similar to the schematic ones of Millener *et al.*[27] ($\alpha^2=1$, $\beta^2=0$) to those where a particle-type transition would dominate (REWIL, ZBMII) ($\beta^2>\alpha^2$), passing through the case where the isoscalar contribution would be absent ($\beta^2=\alpha^2$). This picture is proposed to illustrate roughly the present results. The difficulty in performing calculations in a sufficiently extended basis to account at the same time for pairing effects (important in the present results) and deformation effects (important in those of Adelberger *et al.*), which both tend to reduce the PNC transition amplitudes estimated here, invites us to treat any definite conclusion with caution.

The present results support an interpretation different from the one where the small PNC effect in ^{21}Ne would arise from a delicate cancellation of the large isoscalar and isovector contributions as calculated with the "best" DDH values for the weak coupling constants. The relative (or even complete) suppression of the isoscalar contribution necessarily imposes an upper limit on the isovector contribution and therefore on the πNN coupling constant $h_\pi^{(1)}$. Although the conclusion cannot be as convincing as in ^{18}F, where some

TABLE IX. Physical quantities and theoretical PNC matrix elements necessary for calculating γ circular polarizations and asymmetries for the two PMD cases studied in the $A=36$ cases (see Sec. 5.4). The experimental data are taken from Ref. 132 unless noted otherwise.

Nucleus	^{36}Cl	^{36}Ar
$I_i^{\pi}T_i, E_i$ (MeV)→	2^+1,1.959 MeV→	2^+0, 4.951 MeV→
$I_f^{\pi}T_f, E_f$ (MeV)	2^+1,g.s.	2^+0, 1.97 MeV
$I_i^{\pi}T_i, E_i$ (MeV)→	2^-1,1.951 MeV→	2^-0, 4.974 MeV→
$I_f^{\pi}T_f, E_f$ (MeV)	2^+1,g.s.	2^+0, 1.97 MeV
lifetime (τ_+)	(60±15) fs	≤50 fs
lifetime (τ_-)	(2.6±0.3) ps	(14±5) ps
branching ratio (b_+)	94.4%	15%
branching ratio (b_-)	60%	(4.0±0.9)%
mixing ratio $(\delta_+)_{\text{exp}}$	(−5.2±0.06) or (−0.19±0.06) (Ref. 146)	
mixing ratio $(\delta_+)_{\text{theo}}$	−0.24	0.41
mixing ratio $(\delta_-)_{\text{exp}}$	(−0.10±0.10) (Ref. 146)	
mixing ratio $(\delta_-)_{\text{theo}}$	0.009	
$B(\text{E1})_{\text{exp}}$	1.4×10^{-5}	0.7×10^{-7} (if $\delta_-=0$)
$B(\text{E1})_{\text{theo}}$	0.008	0.0
$B(\text{M2})_{\text{exp}}$	≤25	
$B(\text{M2})_{\text{theo}}$	2.5	0.24
$B(\text{M1})_{\text{exp}}$	0.08 ($\delta_+=-0.2$); 0.003 ($\delta_+=-5.2$)	0.6 (if $\delta_+=0$)
$B(\text{M1})_{\text{theo}}$	0.14	0.0009
$B(\text{E2})_{\text{exp}}$	12 ($\delta_+=-0.2$); 298 ($\delta_+=-5.2$)	
$B(\text{E2})_{\text{theo}}$	30	0.27
$M_{\text{PNC}}^{\text{DDP}}$ (eV)	−0.019	0.122
$M_{\text{PNC}}^{\text{DDH}}$ (eV), $h_\pi^1=\frac{1}{4}(h_\pi^1)_{\text{DDH}}$	−0.057	0.122
$M_{\text{PNC}}^{\text{KM}}$ (eV)	−0.023	0.067
f	8.3	32.4
F	2000	2400

check is possible from the β decay of ^{18}Ne, a similar limit, $h_\pi^{(1)}<0.15\cdot10^{-6}$, is obtained. An even lower limit could be obtained if the isoscalar contribution was shown to be totally absent in the present PNC transition.

While a low value for $h_\pi^{(1)}$ is quite consistent with DDH expectations, it presupposes inputs that are far from what could be considered as the best ones at the present time: the absence of strange content in the nucleon, and the absense of strong-interaction effects in building the effective quark interaction. In our opinion, the explanation for a low value of $h_\pi^{(1)}$ should be rather found in the contributions which were considered negligible until now and, in any case, difficult to estimate.

5.4. Parity-mixed doublet in $A=36$ nuclei

There is another pair of PMDs which can be described approximately with the same strong-interaction models: one PMD, first proposed by Dumitrescu and Stratan,[46] belongs to the ^{36}Cl energy spectrum, and another to that of ^{36}Ar (see Tables I and IX and Ref. 132). Neglecting in the ^{36}Cl case the isotensor contribution, we are dealing with two dominant contributions of opposite sign, one isovector and one isoscalar, while the ^{36}Ar case is a pure isoscalar one. The last two PMDs are analogous to the ^{18}F–^{19}F case. For example, the ^{36}Ar PMD can be populated in the ^{39}K$(\vec{p},\alpha)^{36}$Ar reaction ($E_p\approx3.7$ MeV) in analogy with the ^{19}F case, while the ^{36}Cl PMD can be populated in the ^{39}K$(\vec{n},\alpha)^{36}$Cl reaction ($E_n\approx0.6$ MeV).

The calculations of the PNC matrix element were carried out with the shell-model code OXBASH[63] in the sd–pf model space in which the $2s_{1/2}$, $1d_{5/2}$, $1d_{3/2}$, $2p_{1/2}$, $2p_{3/2}$, $1f_{7/2}$, and $1f_{5/2}$ orbitals are active. The truncations that we made within this model space were $(1d_{5/2})^{12}(2s_{1/2}-1d_{3/2})^8$ for the positive-parity states and $(2s1d)^{19}(2p1f)^1$ for the negative-parity states [$(0+1)\hbar\omega$ calculations]. These truncations are necessary, owing to the dimension limitations, but we believe that they are realistic. The Brown–Wildenthal interaction[143] was used for the positive-parity states, and the WBMB interaction[144] was used for the negative-parity states. Both interactions have been tested extensively with regard to their reproduction of spectroscopic properties.[143,144] The calculation of the PNC matrix element which included both the core (inactive) and active orbitals has been performed as described in Ref. 25.

All the components[13,16] of the parity-nonconserving potential are short-range two-body operators. Because the behavior of the shell-model wave functions at small NN distances has to be modified, short-range correlations (SRC) were included by multiplying the harmonic-oscillator wave functions (with $\hbar\omega=45\cdot A^{-1/3}$ MeV$-25\cdot A^{-2/3}$ MeV) by the Miller and Spencer factor.[65] This procedure is consistent with results obtained by using more elaborate treatments of SRC such as the generalized Bethe–Goldstone approach.[66,67] The PNC pion-exchange matrix is decreased by 30–50% as compared with the values of the matrix elements without SRC, while the $\rho(\omega)$-exchange matrix elements are much smaller (by a factor of 1/3–1/6).

The Horoi[47] values calculated for the excitation energies of the first three 2^+ $T=0$ levels in ^{36}Ar are 1.927, 4.410, and 7.174 MeV. The first two are in good agreement with experimental levels at 1.970 and 4.440 MeV. The third 2^+0 $E_x=4.951$ MeV state (belonging to the parity doublet) is apparently an intruder in the $2s1d$ $(0\hbar\omega)$ configuration. This conclusion is also supported by the suppressed β transition probability.[145] Horoi included the $2\hbar\omega$ configurations in a rather reduced space (the $1d_{5/2}$ orbital is frozen and the $1f_{1/2}$ orbital is not allowed), which we consider adequate for this problem. The $2\hbar\omega$ configurations have been shifted down by 11.5 MeV, so that the first 2^+0 state with a dominant $2\hbar\omega$ component (~80%) becomes the third 2^+0 state in the calculated spectrum. The dominant PNC transition is $1d_{3/2}-2p_{3/2}$, and the PNC matrix element is 0.122 eV (see Table I). We should mention that this value is more uncertain than the ^{36}Cl value because the third 2^+0 state cannot be described either as a pure $0\hbar\omega$ configuration or as a pure $2\hbar\omega$ configuration. In the ^{36}Cl case, the positive-parity states are in very good agreement with experiment (e.g., the second 2^+ state has a theoretical energy 2.004 MeV, compared with the experimental value of 1.96 MeV). The theoretical $B(\text{E}\lambda)$ and $B(\text{M}\lambda)$ and the mixing ratios are in relatively good agreement with experiment (see Table IX) in both cases.

The results (up to a complex phase factor) can be summarized as follows:

$$M_{\mathrm{PNC}}(^{36}\mathrm{Cl}) = (1.094\cdot h_{\pi}^{(1)} - 0.205\cdot h_{\rho}^{(1)} - 0.304\cdot h_{\omega}^{(1)} - 0.027\cdot h_{\rho'}^{(1)} + 0.569\cdot h_{\rho}^{(0)} + 0.323\cdot h_{\omega}^{(0)} + 0.015\cdot h_{\rho}^{(2)})\cdot 10^{-2}\ \mathrm{eV}, \quad (60)$$

$$M_{\mathrm{PNC}}(^{36}\mathrm{Ar}) = -(0.995\cdot h_{\rho}^{(0)} + 0.443\cdot h_{\omega}^{(0)})\cdot 10^{-2}\ \mathrm{eV}. \quad (61)$$

Here $h_{\mathrm{meson}}^{\Delta T}$ should be given in units of 10^{-7}, as in Table II.

6. CONCLUSIONS

The PNC nuclear-physics processes determined by the isovector part of the weak hadron–hadron interaction are important for studies of the neutral currents.

Our understanding of the $\Delta S=0$ hadronic weak interaction is based on a small collection of high-precision experiments (see the review of Ref. 16) on the two-nucleon system and light nuclei which isolate the weak interaction via its parity-nonconserving signature. The experiments have yielded significant but incomplete information on the weak meson–nucleon coupling constants, which are in qualitative agreement with predictions[13,14] based on the standard model, although the pion coupling ($h_{\pi}^{(1)}$) is much smaller than expected. Unfortunately, the measured observables need a complicated theoretical interpretation, and the extraction of the weak meson–nucleon couplings from experiment is not model-independent at present. Owing to the generally small values of most of the terms contributing to the PNC matrix elements, the PNC in dealing with the low-energy nuclear spectrum should essentially involve the strength of the nucleon–nucleus weak force. As weak interactions do not conserve the isospin, this strength can be characterized by two numbers, referring to the proton and neutron forces, respectively, or, equivalently, to their isovector and isoscalar components. Moreover, the main contribution coming from the isovector part is assumed to be due to the one-pion exchange term (the long-range term), while the main contribution coming from the isoscalar part is assumed to be due to the ρ-meson exchange term (the short-range term). At present one cannot devise any experiment that would be sensitive to other contributions to the weak hadron–hadron interaction potential. Therefore, in principle two independent experiments should be sufficient for the determination of the above nucleon–nucleus weak forces. For that reason, in this work we tried to select pairs of experiments for which one uses more or less the same theoretical treatment. We investigated the possibility of extracting from experiment the necessary information on the neutral-current contributions to the structure of the weak interactions that violate the parity-conservation law. The low-energy nuclear-physics processes considered here were resonance nuclear scattering and reactions induced by polarized protons, emission of polarized gamma rays from oriented and nonoriented nuclei, and parity-forbidden alpha decay. Some comments on the PNC nucleon–nucleon (PNC-NN) interaction have been presented. Applications for specific scattering, reaction, and decay modes have been given. New experiments are proposed. The most favorable case that we consider is the neutral-current investigation via the $^{15}\mathrm{N}(\vec{p},\alpha)^{12}\mathrm{C}$ resonance reaction that populates the 13-MeV, $J^{\pi}=2^{\pm}$ isovector parity-mixed doublet. The energy anomalies for the expected interference effects, relevant for the experiments, have been found to be $A_L=1.4\times10^{-5}$ and $A_b=1.4\times10^{-5}$ at $\theta=150°$ and are based on the conservative value of 0.1 eV for the PNC matrix element. Such an experiment together with the PNC α-decay experiment (an isoscalar case)[45] would fix from experiment the isoscalar and isovector strengths of the H_{PNC} interaction.

We reexamined estimates of the circular polarization of γ rays emitted in the transition $1/2^-$, $T=1/2$ (2.789 MeV)$\rightarrow 3/2^+$, $T=1/2$ (g.s) in ^{21}Ne, which involves the parity admixture of two closed states $1/2^-$, $T=1/2$ (2.789 MeV) and $1/2^+$, $T=1/2$ (2.796 MeV). New estimates have been added to previous ones. From the study a different interpretation of the measurement is suggested. In contrast to the previous claim by Brandenburg *et al.*,[28] we found that the isovector contribution is well defined in sign, while the isoscalar contribution is not and is somewhat disfavored. This conclusion agrees with the recent result of Ref. 43 based on a much larger valence basis. Unfortunately, a more precise experiment (using Compton polarimeters) than those already carried out[16] is at present impossible to perform.

The author would like to thank Professor Luciano Fonda for his constant encouragement, Professor B. Desplanques, P. G. Bizzeti, and G. Clausnitzer for fruitful discussions during his visits to the University of Florence, the University of Giessen, and the Institute for Nuclear Sciences at Grenoble, respectively, Professor B. Alex Brown for providing the OXBASH code and for interesting discussions, and Dr. M. Horoi for many years of collaboration. He would also like to thank Professor Abdus Salam, the International Atomic Energy Agency, and UNESCO for hospitality at the International Centre for Theoretical Physics, Trieste.

[1] S. A. Bludman, Nuovo Cimento G, 433 (1958).
[2] S. L. Glashow, Nucl. Phys. **22**, 579 (1961).
[3] A. Salam and J. C. Ward, Phys. Rev. Lett. **13**, 168 (1964).
[4] S. Weinberg, Phys. Rev. Lett. **19**, 1264 (1967).
[5] P. W. Higgs, Phys. Rev. Lett. **13**, 508 (1964).
[6] F. Englert and R. Brout, Phys. Rev. Lett. **13**, 321 (1964).
[7] A. Salam, in *Elementary Particle Theory*, edited by N. Svartholm (Almqvist and Wiskel, Stockholm, 1968), p. 367.
[8] F. J. Hasert *et al.*, Phys. Lett. B **46**, 138 (1973).
[9] G. Arnison *et al.*, UA-1 Collaboration, Phys. Lett. B **122**, 103 (1983).
[10] M. Banner *et al.*, UA-2 Collaboration, Phys. Lett. B **122**, 476 (1983).
[11] S. L. Glashow, G. Iliopoulos, and L. Maiani, Phys. Rev. D **2**, 1285 (1970).
[12] M. Kobayashi and T. Maskawa, Prog. Theor. Phys. **49**, 652 (1973).
[13] B. Desplanques, J. F. Donoghue, and B. R. Holstein, Ann. Phys. (N.Y.) **124**, 449 (1980).
[14] V. M. Dubovik and S. V. Zenkin, Ann. Phys. (N.Y.) **172**, 100 (1986); V. M. Dubovik, S. V. Zenkin, I. T. Obukhovskiĭ, and L. A. Tosunyan, Fiz. Élem. Chastits At. Yadra **18**, 575 (1987) [Sov. J. Part. Nucl. **18**, 244 (1987)].
[15] N. Kaiser and U. G. Meissner, Nucl. Phys. **A489**, 671 (1988); **A499**, 699 (1989); **A510**, 759 (1990); Mod. Phys. Lett. **A5**, 1703 (1990).
[16] E. G. Adelberger and W. C. Haxton, Ann. Rev. Nucl. Part. Sci. **35**, 501 (1985).
[17] P. G. Bizzeti, Riv. Nuovo Cimento **6**, No. 12, 1 (1983).
[18] E. G. Adelberger, M. M. Hindi, C. D. Hoyle, H. E. Swanson, R. D. Von Lintig, and W. C. Haxton, Phys. Rev. C **27**, 2833 (1983).
[19] K. Elsener, W. Gruebler, V. Koenig, C. Schweitzer, P. A. Schmeltzbach, J. Ulbricht, F. Sperisen, and M. Merdzan, Phys. Lett. B **117**, 167 (1982); Phys. Rev. Lett. **52**, 1476 (1984).
[20] S. Popescu, O. Dumitrescu, and J. P. Vary, to be published in Phys. Rev. C.
[21] V. E. Bunakov, Fiz. Élem. Chastits At. Yadra **26**, 285 (1995) [Phys. Part. Nucl. **26**, 115 (1995)].

[22] O. Dumitrescu, Preprint IC/95/139, ICTP, Trieste (1995); submitted for publication in Fiz. Elem. Chastits At. Yadra.
[23] B. Desplanques, in *Proceedings of the 8th International Workshop on Weak Interactions and Neutrinos*, Javea, 1982, edited by A. Morales (Singapore, 1983), p. 515; *Proceedings of the International Workshop on Reactors Based on Fundamental Physics*, Grenoble, 1983; J. Phys. (Paris) **45**, C3–55 (1984).
[24] W. C. Haxton, B. F. Gibson, and E. M. Henley, Phys Rev. Lett. **45**, 1677 (1980).
[25] B. A. Brown, W. A. Richter, and N. S. Godwin, Phys. Rev. Lett. **45**, 1681 (1980).
[26] K. A. Snover *et al.*, Phys. Rev. Lett. **41**, 145 (1978); E. D. Earle *et al.*, Nucl. Phys. **A396**, 221c (1983).
[27] D. J. Millener *et al.*, Phys. Rev. C **18**, 1878 (1978).
[28] R. A. Brandenburg *et al.*, Phys. Rev. Lett. **41**, 618 (1978).
[29] B. Desplanques and O. Dumitrescu, Nucl. Phys. **A565**, 818 (1993).
[30] O. Dumitrescu and G. Clausnitzer, Nucl. Phys. **A552**, 306 (1993).
[31] N. Kniest, E. Huettel, E. Pfaff, G. Reiter, and G. Clausnitzer, Phys. Rev. C **41**, 1337 (1990).
[32] N. Kniest, E. Huettel, E. Pfaff, G. Reiter, G. Clausnitzer, P. G. Bizzeti, P. Maurenzig, and N. Taccetti, Phys. Rev. C **27**, 906 (1983).
[33] J. Ohlert, O. Traudt, and H. Waeffler, Phys. Rev. Lett. **47**, 475 (1981).
[34] N. Kniest, M. Horoi, O. Dumitrescu, and G. Clausnitzer, Phys. Rev. C **44**, 491 (1991).
[35] O. Dumitrescu, Nucl. Phys. **A535**, 94 (1991).
[36] A. Redder *et al.*, Z. Phys. A **305**, 325 (1982).
[37] O. Dumitrescu, M. Horoi, F. Carstoiu, and Gh. Stratan, Phys. Rev. C **41**, 1462 (1990).
[38] M. Preiss, R. Baumann, F. Cârstoiu, C. Doerrenbach, R. Euler, S. Heine, M. Horoi, G. Keil, M. Mildner, E. Pfaff, O. Dumitrescu, and G. Clausnitzer, in *Proc. of the Salzburg Meeting on Nuclear Physics* (1992).
[39] M. Horoi, G. Clausnitzer, B. A. Brown, and E. K. Warburton, Phys. Rev. C **50**, 775 (1994).
[40] I. Brandus, F. Carstoiu, O. Dumitrescu, M. Horoi, and F. Nichitiu, Rev. Roum. Phys. **36**, 135 (1991).
[41] D. Mihailescu and O. Dumitrescu, Rom. Rep. Phys. **45**, 661 (1993).
[42] D. Mihailescu, H. Comisel, and O. Dumitrescu, Rom. J. Phys. **39**, 223 (1993).
[43] M. Horoi, G. Clausnitzer, B. A. Brown, and E. K. Warburton, NATO–ASI Ser. B Phys. **334** (1994); M. Horoi and B. A. Brown, Phys. Rev. Lett. **74**, 231 (1995).
[44] F. Carstoiu, O. Dumitrescu, G. Stratan, and M. Braic, Nucl. Phys. **A441**, 221 (1985).
[45] K. Neuebeck, H. Schober, and H. Waeffler, Phys. Rev. C **10**, 320 (1974).
[46] O. Dumitrescu and G. Stratan, Nuovo Cimento A **105**, 901 (1991).
[47] M. Horoi, Phys. Rev. C **50**, 2392 (1994).
[48] C. M. Frankle, J. D. Bowman, J. E. Bush, P. P. J. Delheij, C. R. Gould, D. G. Haase, J. N. Knudson, G. E. Mitchell, S. Pentila, H. Postma, N. R. Robertson, S. J. Seestrom, J. J. Szymanski, S. H. Yoo, V. W. Yuan, and X. Zhu, Phys. Rev. C **46**, 778 (1992).
[49] C. A. Barnes, M. M. Lowry, J. H. Davidson, R. E. Mars, F. B. Morinigo, B. Chang, E. G. Adelberger, and H. E. Swanson, Phys. Rev. Lett. **40**, 840 (1979).
[50] H. B. Mak, H. C. Evans, G. T. Ewan, J. R. Leslie, J. D. MacArthur, W. McLachtie, B. C. Robertson, P. Skensved, S. A. Mann, A. B. McDonald, and C. A. Barnes, Reports on Research in Nuclear Physics at Queens University (Kingston, Ont., 1981), p. 19.
[51] M. Bini, T. F. Fazzini, G. Poggi, and N. Taccetti, Phys. Rev. C **38**, 1195 (1988); Phys. Rev. Lett. **55**, 795 (1985).
[52] P. G. Bizzeti, T. F. Fazzini, P. R. Maurenzig, A. Perego, G. Poggi, P. Sona, and N. Taccetti, Lett. Nuovo Cimento **29**, 167 (1980); P. R. Maurenzig, M. Bini, P. G. Bizzeti, T. F. Fazzini, A. Perego, G. Poggi, P. Sona, and N. Taccetti, in *Proceedings of the 1979 International Conf. on Neutrinos, Weak Interactions and Cosmology*, Vol. 2, edited by A. Haatuft and C. Jarlskog (Bergen, 1979), p. 97; M. Bini, P. G. Bizzeti, and P. Sona, Phys. Rev. C **23**, 1265 (1981); Lett. Nuovo Cimento **41**, 191 (1984).
[53] G. Afrens, W. Harfst, J. R. Kass, E. V. Mason, H. Schober, G. Stefens, and H. Waeffler, Nucl. Phys. **A390**, 486 (1982).
[54] P. G. Bizzeti, Phys. Rev. C **33**, 1837 (1986).
[55] E. G. Adelberger, P. Hoodbhoy, and B. A. Brown, Phys. Rev. C **30**, 456 (1984); **33**, 1840 (1986).
[56] V. J. Zeps, Ph.D. Thesis, University of Washington (1989); V. J. Zeps, E. G. Adelberger, A. Garcia, C. A. Gossett, H. E. Swanson, W. Haeberli, P. A. Quin, and J. Sromicki, AIP Conf. Proc. **176**, 1098 (1989); H. E. Swanson, V. J. Zeps, E. G. Adelberger, C. A. Gossett, J. Stromecki, W. Haerberli, and P. Quin, Heidelberg Conf. Proc., 648 and 277 (1986); *Weak and Electromagnetic Interactions in Nuclei*; edited by H. V. Klapdoor and J. Metzinger.
[57] M. Bini, P. G. Bizzeti, and P. Sona, Phys. Rev. C **23**, 1265 (1980).
[58] R. E. Karlsen, Europhys. Lett. **22**, 341 (1993).
[59] E. M. Henley, W.-Y. P. Hwang, and L. S. Kisslinger, to be published in Phys. Lett.
[60] E. M. Henley and J. Pasupathy, Nucl. Phys. **A556**, 467 (1993); E. M. Henley, W.-Y. P. Hwang and L. S. Kisslinger, Phys. Rev. D **46** 431 (1992); T. Hatsuda *et al.*, Phys. Rev. C **49**, 452 (1993); L. J. Reinders, H. Rubinstein, and S. Yazaki, Nucl. Phys. **B213**, 109 (1983).
[61] I. Grach and Shmatikov, ITEP Preprint 100-88 (1988).
[62] V. M. Khatsimovskii, Preprint 84-164 Novosibirsk; Yad. Fiz. **42**, 1236 (1985) [Sov. J. Nucl. Phys. **42**, 781 (1985)].
[63] B. A. Brown, A. Etchegoyen, and W. D. M. Rae, MSU–NSCL Report **524** (1985); B. A. Brown, W. E. Ormand, J. S. Winfield, L. Zhao, A. Etchegoyen, W. M. Rae, N. S. Godwin, W. A. Richter, and C. D. Zimmerman, MSU–NSLL Report, Michigan State University version of the OXBASH code **524** (1988); B. A. Brown and B. H. Wildenthal, Ann. Rev. Nucl. Part. Sci. **38**, 29 (1988).
[64] F. Ajzenberg-Selove, Nucl. Phys. **A499**, 1 (1987) (A=13–15); **A475**, 1 (1987) (A=18–20); **A460**, 1 (1986) (A=16,17); **A433**, 1 (1985) (A=11,12); **A320**, 1 (1979) (A=5–10); **A281**, 1 (1977) (A=16,17).
[65] G. A. Miller and J. E. Spencer, Ann. Phys. (N.Y.) **100**, 562 (1976).
[66] O. Dumitrescu, M. Gari, H. Kuemmel, and J. G. Zabolitzky, Z. Naturforsch. A **27**, 733 (1972); Phys. Lett. B **35**, 19 (1971).
[67] M. Gari, Phys. Rep. C **6**, 317 (1973).
[68] R. Machleidt, K. Holinde, and Ch. Elster, Phys. Rep. **149**, 1 (1987); R. Machleidt, Adv. Nucl. Phys. **19**, 189 (1989).
[69] M. Lacomb *et al.*, Phys. Rev. C **21** 861 (1980).
[70] M. F. Gari and W. Kruempelmann, Z. Phys. A **322**, 689 (1985); Phys. Lett. B **173**, 10 (1986); S. Deister, M. F. Gari, W. Kruempelmann, and M. Mahlke, Few-Body Systems **10**, 1 (1991).
[71] T. T. S. Kuo and G. E. Brown, Nucl. Phys. **85**, 40 (1966).
[72] T. T. S. Kuo, Ann. Rev. Nucl. Part. Sci. **24**, 101 (1974); Nucl. Phys. **A103**, 71 (1967).
[73] O. Dumitrescu, in *Proc. of the Predeal Summer School "Recent Advances in Nuclear Structure,"* edited by D. Bucurescu, G. Cata-Danil, and N. V. Zamfir (World Scientific, Singapore, 1991), p. 359.
[74] B. D. Day, Rev. Mod. Phys. **39**, 719 (1967); **50**, 495 (1978).
[75] R. Rajaraman and H. A. Bethe, Rev. Mod. Phys. **39**, 745 (1967).
[76] A. P. Zuker, B. Buck, and J. B. McGrory, Phys. Rev. Lett. **21**, 39 (1968).
[77] A. P. Zuker, Phys. Rev. Lett. **23**, 983 (1969).
[78] B. S. Reehal and B. H. Wildenthal, Part. Nucl. **6**, 137 (1973).
[79] N. Tanner, Phys. Rev. **107**, 1203 (1957).
[80] R. P. Feynman and M. Gell-Mann, Phys. Rev. **109**, 193 (1958).
[81] V. M. Lobashov, V. A. Nazarenko, L. F. Saenko, L. F. Smotriskiĭ, and O. I. Kharkevith, JETP Lett. **5**, 59 (1967); Phys. Lett. **25**, 104 (1967).
[82] G. Barton, Nuovo Cimento **19**, 512 (1961).
[83] T. H. R. Skyrme, Proc. R. Soc. London Ser. A **260**, 127 (1961).
[84] E. Witten, Nucl. Phys. **B223**, 422, 433 (1983).
[85] U.-G. Meissner, Phys. Rep. **161**, 213 (1988).
[86] I. Zahed and G. E. Brown, Phys. Rep. **142**, 1 (1986).
[87] B. Schwesinger, H. Weigel, G. Holzwarth, and A. Hayashi, Phys. Rep. **173**, 173 (1989).
[88] U.-G. Meissner and I. Zahed, Adv. Nucl. Phys. **17**, 143 (1986).
[89] G. Holzwarth and B. Schwesinger, Rep. Prog. Phys. **49**, 825 (1986).
[90] H. A. Bethe, Ann. Rev. Nucl. Sci. **21**, 93 (1971).
[91] E. Feenberg, *Theory of Quantum Fluids* (Academic Press, New York, 1969).
[92] E. D. Cummings and P. H. Bucksbaum, *Weak Interactions of Leptons and Hadrons* (Cambridge University Press, Cambridge, 1983).
[93] J. F. Donoghue, E. Golowich, and B. R. Holstein, Phys. Rep. **131**, Nos. 5 and 6, 319 (1980).
[94] E. M. Henley, Phys. Lett. B **28**, 1 (1968); Ann. Rev. Nucl. Sci. **19**, 367 (1969).
[95] B. R. Holstein, *Weak Interactions in Nuclei* (Princeton Series in Physics, 1989).
[96] I. Caprini and L. Micu, Phys. Rev. C **37**, 2209 (1988); Phys. Lett. B **153**, 8 (1985).
[97] C. Itzykson and J. B. Zuber, *Introduction to Quantum Field Theory* (McGraw-Hill, New York, 1980).

[98] D. Walecka, Ann. Phys. (N.Y.) **83**, 491 (1974); B. D. Serot, Nucl. Phys. **A446**, 97c (1983).
[99] H. Kuemmel, Nucl. Phys. **A146**, 205 (1971).
[100] H. Kuemmel, K. H. Luermann, and J. G. Zabolitzky, Phys. Rep. **36**, 1 (1978).
[101] J. M. Irvine, Rep. Prog. Phys. **51**, 1181 (1988).
[102] A. Kallio and B. D. Day, Phys. Lett. B **25**, 72 (1967); Nucl. Phys. **A124**, 177 (1968).
[103] R. V. Reid, Jr., Ann. Phys. (N.Y.) 50, 411 (1968).
[104] B. S. Reehal and B. H. Wildenthal, Part. Nucl. **6**, 137 (1973).
[105] S. Cohen and D. Kurath, Nucl. Phys. **A73**, 1 (1965).
[106] O. Preedom and B. H. Wildenthal, Phys. Rev. C **6**, 1633 (1972).
[107] D. J. Millener and D. Kurath, Nucl. Phys. **A255**, 315 (1975).
[108] See, for example, J. H. Wilkinson, *The Algebraic Eigenvalue Problem* (Clarendon Press, Oxford, 1965).
[109] R. R. Whitehead, in *Moment Methods in Many Fermion Systems*, edited by B. J. Dalton, S. M. Grimes, J. P. Vary, and S. A. Williams (Plenum Press, New York, 1980), p. 235.
[110] M. Horoi, B. A. Brown, and V. Zelevinsky, Phys. Rev. C **50**, R2274 (1994).
[111] B. A. Brown, R. Rahdi, and B. H. Wildenthal, Phys. Rep. **101**, 313 (1983).
[112] J. B. McGrory and B. H. Wildenthal, Phys. Rev. C **7**, 954 (1973); Ann. Rev. Nucl. Sci. **30**, 383 (1980).
[113] B. A. Brown and B. H. Wildenthal, Ann. Rev. Nucl. Part. Sci. **38**, 29 (1988); Phys. Lett. B **198**, 29 (1987); Phys. Rev. C **27**, 1296 (1983).
[114] B. H. Wildenthal, Prog. Part. Nucl. Phys. **11**, 5 (1984); Phys. Rev. Lett. **33**, 233 (1974).
[115] K. K. Seth *et al.*, Phys. Rev. Lett. **33**, 233 (1974).
[116] P. Federman and S. Pittel, Phys. Rev. **186**, 1106 (1969).
[117] B. A. Brown *et al.*, Ann. Phys. (N.Y.) **182**, 191 (1988).
[118] D. H. Gloekner and D. R. Lawson, Phys. Lett. B **53**, 313 (1974).
[119] V. G. Soloviev, *Theory of Complex Nuclei* (Pergamon Press, New York, 1976) [Russ. original, Nauka, Moscow, 1971].
[120] C. Mahaux and H. A. Weidenmueller, *Shell Model Approach to Nuclear Reactions* (North-Holland, Amsterdam, 1969).
[121] M. Preiss and G. Clausnitzer, NATO-ASI Ser. B Phys. **334**, 353 (1994).
[122] W. Biesiot and Ph. B. Smith, Phys. Rev. C **24**, 2443 (1981).
[123] P. G. Bizzeti and P. R. Maurenzig, Nuovo Cimento A **56**, 492 (1980).
[124] K. S. Krane, C. E. Olsen, J. R. Sites, and W. A. Steyert, Phys. Rev. C **4**, 1906 (1971).
[125] M. Dahlinger, E. Kankeleit, D. Habs, D. Schwalm, B. Schwartz, R. S. Simon, J. D. Burrows, and P. A. Butler, Nucl. Phys. **A484**, 337 (1988).
[126] G. H. Pepper and L. Brown, Nucl. Phys. **A260**, 163 (1976); K. H. Bray, A. D. Frawley, T. R. Opfel, and F. R. Barker, Nucl. Phys. **A288**, 334 (1977).
[127] W. C. Haxton, private communication.
[128] W. C. Haxton, in *Proc. of the Symp./Workshop on Spin Symmetry*, edited by W. D. Ramsay and W. T. H. van Oers (1989), p. 13.
[129] G. J. Wagner, K. T. Knoeple, G. Mairle, P. Doll, and H. Hafner, Phys. Rev. C **16**, 1271 (1977).
[130] R. A. Leavit, H. C. Evans, G. T. Evan, H. B. Mak, R. E. Azuma, C. Rolfs, and K. P. Jackson, Nucl. Phys. **A410**, 83 (1983).
[131] E. Browne, Nucl. Data Sheets **52**, 127 (1987).
[132] D. M. Endt, Nucl. Phys. **A521**, 1 (1990).
[133] R. J. Blin-Stoyle, *Fundamental Interactions and the Nucleus* (North-Holland, Amsterdam, 1973).
[134] A. Bohr and B. R. Mottelson, *Nuclear Structure* (Benjamin, New York, 1975).
[135] M. Gari, J. B. McGrory, and R. Offerman, Phys. Lett. B **55**, 277 (1975).
[136] F. C. Michel, Phys. Rev. **133**, B329 (1964).
[137] B. Desplanques and J. Missimer, Nucl. Phys. **A300**, 286 (1978); B. Desplanques, Nucl. Phys. **A242**, 423 (1975).
[138] B. Desplanques, Nucl. Phys. **A316**, 244 (1979).
[139] M. Chemtob and B. Desplanques, Nucl. Phys. **B78**, 139 (1974).
[140] M. Gari and J. H. Reid, Phys. Lett. B **53**, 237 (1974).
[141] B. Desplanques *et al.*, Z. Phys. C **51**, 499 (1991); J. Bernabeu *et al.*, Z. Phys. C **46**, 323 (1990).
[142] B. Desplanques, Nucl. Phys. **A335**, 147 (1980).
[143] B. A. Brown and B. H. Wildenthal, Ann. Rev. Nucl. Part. Sci. **38**, 29 (1988).
[144] E. K. Warburton, J. A. Becker, and B. A. Brown, Phys. Rev. C **41**, 1147 (1990).
[145] B. A. Brown and B. H. Wildenthal, At. Data Nucl. Data Tables **33** (1985).
[146] A. M. Spits and J. Kopecky, Nucl. Phys. **A521**, 1 (1990).

This article was published in English in the original Russian journal. It is reproduced here with the stylistic changes by the Translations Editor.